EFFECTS OF HSA21 GENE EXPRESSION ON EARLY VERTEBRATE DEVELOPMENT

by
Sarah McGuire Edie

A dissertation submitted to Johns Hopkins University in conformity with the requirements for the degree of Doctor of Philosophy

Baltimore, Maryland
April, 2014

ABSTRACT:

Trisomy for human chromosome 21 (Hsa21) results in Down Syndrome (DS), one of the most genetically complex conditions that is compatible with human survival. Up to half of DS conceptions do not survive to term. Effects of over-expression of individual Hsa21 genes that occur during embryogenesis are difficult to study in mammals. We created a gene expression set of 171 Hsa21 cDNAs. RNA was transcribed from cDNA and injected into 1-2 cell zebrafish embryos which were screened at 5 days post-fertilization for gross morphological effects. Twenty-three genes gave an initial phenotype and ten of those genes robustly recapitulated the phenotype in subsequent experiments. Seven of these gave a phenotype consistent with down regulation of the sonic hedgehog (Shh) pathway, two showed a phenotype that indicated involvement of neural crest cells, and one showed pericardial edema. We performed combinatorial injections with multiple Hsa21 genes and found both additive and compensatory effects. This system and gene set supports many types of examination of multiple gene effects on early vertebrate development that are relevant to DS.

Readers:

Roger Reeves, PhD

Valerie DeLeon, PhD

ACKNOWLEDGMENTS

I would like to thank all those you helped me to achieve my dream of obtaining a PhD in Human Genetics.

To begin with, I would like to thank Roger Reeves for his wonderful mentorship and all the advice that he's given me. He's suffered through my endless questions and enthusiasm, even when said questions/enthusiasm was for projects other than my thesis. He's helped me when my fish didn't lay and I was endlessly frustrated; and he's been there when I discovered a new cool phenotype I hadn't seen before.

I would like to thank the students and faculty of the McKusick-Nathans Institute of Genetic Medicine, the predoctoral training program in human genetics and in particular Sandy Muscelli, Dave Valle and Kirby Smith for all their support, advice and friendship. Sandy, with her bowl of candy for the student studying for quals; Dave and Kirby for their advice and their extensive knowledge and interest in extending that knowledge to students. I would like to thank my fellow classmates who've studied, sweated and sweared during our years of classes; who are among the few people to know what going through this process really entails.

I would like to thank my friends and family who've been there for me through everything, even when I talked science till I was blue in the face. Even when they didn't understand the problem, they always listened and tried to help me figure out the solution. My mom, I love you to the stars and back. My dad, who I can count on to always be proud of me, wherever I go. My brother, who is always there to laugh with me, and sometimes at me. My grandmother who is one of the strongest people I know and is for whom learning and education is so important.

Lastly, but most importantly, my husband Chris and my son Booker. I did this for me primarily, but also mostly for you. You pushed me and helped me and were there for me during all the best times of my life.

TABLE OF CONTENTS

LIST OF TABLES:

LIST OF FIGURES:

CHAPTER 1: INTRODUCTION

History of DS

In 1838, Étienne Esquirole described a congenital form of cognitive impairment in a number of patients that included a physical description of short stature and a broad flattened nose, which is the first description of Trisomy 21 [1]. Edouard Séguin, in 1846, expanded upon Esquirole's observations with a description of open mouth and thick protruding tongue [2,3]. In an essay written in 1866, J. Langdon Down discussed a population of individuals with congenital cognitive impairment, as well as characteristic facial features [4]. DS was found to be caused by trisomy of human chromosome 21 (Hsa21) in 1959 by Lejeune, Gautier and Turpin [2]. In 1961, the condition that was independently described by Esquirole, Séguin and Down would be renamed Down Syndrome (DS), and is now also referred to as Trisomy 21 [2].

Clinical features of DS

The initial features described by Esquirole, Séguin and Down centered around the facial features and the cognitive impairment. Now, DS is recognized as having >80 clinical features, including cognitive impairment, short stature, and characteristic facial features [5]. These features affect many systems and vary in penetrance and expressivity. Many features occur at birth and during early infancy, such as the facial features and the increased risk of congenital heart defects and Hirschprung's disease; others occur later, such as the increased risk of Alzheimer's disease [6].

The variability of penetrance and expressivity of the phenotypes associated with DS has led to the hypothesis that although trisomy 21 is a large risk factor for the development of these phenotypes, it is not sufficient for some of these phenotypes, meaning that there are modifiers of the DS phenotypes [7]. These modifiers may interact with one or a few genes on Hsa21. Understanding how the different genes on Hsa21 may contribute to the different phenotypes associated with DS will help in the pursuit of therapeutic targets for ameliorating the condition.

Genetic content of Hsa21

It was first suggested that Down Syndrome was caused by a chromosomal abnormality in 1932 by both Waardenburg as well as independently by Davenport [8,9]. In 1959, the chromosomal basis for Down Syndrome was established by Lejeune, Gautier and Turpin, who used cytogenic techniques to determine that individuals with Down Syndrome had an extra copy of chromosome 21 [2]. The nearly complete DNA sequence of Hsa21 was published in May of 2000, with an estimate of 225 genes and 59 pseudogenes [10].

Hsa21 is one of the smallest autosomes with an approximately 33.6 MB long arm, representing ~1% of the total human genome [7]. Since the original publication, estimates of the genetic content of Hsa21 have ranged from ~200-500 genes, with the most recent estimate of 552 genes (excluding KRTAP genes, of which there ~49) [7,10,11,12]. These genes include 161 genes that unambiguously code for proteins, i.e. they have a RefSeq Protein associated, five microRNAs, 250 open reading frames (ORF) in which the ORFS encode a protein >50 amino acids, and 140 ORF with <50 amino acids [12]. In 2007, it

was estimated that of the 430 genes reported, approximately 45% had no identified function [13]. When considering just the genes that are conserved with mouse, ~14% had no functional annotation [11]. Understanding the function and the role these genes may play in the development of DS could lead to identification of pathways and targets for therapeutic treatment.

Creating genotype-phenotype correlations

One method of identifying genes that may play significant roles in the presentation of DS phenotypes is to look at small duplications/trisomies in individuals and compare that to the phenotypes exhibited by those individuals. By examining patients with partial trisomies and correlating the trisomic regions with the presentation of DS phenotypes, researchers determined the location of the so-called "Down Syndrome Critical Region" (DSCR, originally called Down Syndrome Critical Region 1) which includes the region D21S55-MX1 or D21S55-CRYAA1, located at 21q22.2-21q22.3 [14,15]. However, other phenotypic mapping using partial trisomies has indicated that genes outside the D21S55 region also contribute to the DS phenotypes, and individuals with clinical features of DS have been identified who have partial trisomy 21 that does not include D21S55 [16].

Although the DSCR is not responsible for all of the DS phenotypes, the next option is to look for regions that have strong contributions for specific phenotypes. To develop a phenotypic map of Hsa21, Korenberg and colleagues used 16 patients with partial Trisomy 21 to attempt to create a phenotypic map of 25 DS features. Their data suggest

that for most of the DS features, multiple gene clusters contribute to the presentation and variability [16].

Interest in developing a high resolution phenotypic map has not waned. In 2009 Korbel and colleagues [17] made another attempt at a phenotypic map using 30 patients with partial Trisomy 21 and examined 8 major features of DS, including CHD, cognitive impairment, acute megakaryocytic leukemia (AMKL), transient myeloproliferative disorder (TMD), Hirschsprung's disease (HSCR), duodenal stenosis (DST), imperforate anus (IA) and Alzheimer disease (AD). In the case of certain features (namely AMKL, DST, IA) only a single patient was identified with each feature. This limitation in combination with the observation that some of these patients had complex rearrangements involving duplications, deletions and inversions, as well as some tetrasomic regions, makes analysis of the possible critical regions of specific features complicated. The authors determined that a 1.77 MB region of Hsa21 is responsible for the CHD observed in patients. However, not every patient that was trisomic for that region had CHD, indicating that the region is not sufficient to cause CHD.

Another group in the same year attempted a similar study with 19 individuals with partial trisomy 21, investigating 25 DS features [18]. However, for many of the features observed, the patients who had the observed feature didn't overlap in their trisomic regions, and there were many examples of individuals who did overlap who did not have that particular feature.

Although the concept of finding genes that may play larger roles in the development of DS phenotypes is valuable, the message to take away from these studies is that DS is too complex to assign a single causative region or gene to each character. That complexity means that using human patients to model the condition has limitations in the obtaining a large enough sample of individuals with partial trisomy 21 for different regions of the chromosome that would allow for the identification of genes that may have a function in some of the DS features. At the moment, there aren't enough partial trisomy 21 patients to adequately develop a comprehensive phenotype map, and although that might change in the future; at present, animal models are a better option for these types of studies.

Modeling DS in mice

Understanding how Hsa21 genes function during embryogenesis and how trisomy of those genes cause DS phenotypes is not something that can be undertaken in a comprehensive manner in humans. Animal models are necessary to elucidate the manner in which trisomy 21 causes DS. The best known and most widely used models of DS are available in the mouse. Mice make for a useful model due to the extensive conserved synteny between human and mouse chromosomes. Hsa21 (33.5 Mb) has conserved synteny with mouse chromosomes 10 (2.3 Mb), 16 (23.2 Mb) and 17 (1.1 Mb; Mmu10, Mmu16 and Mmu17 respectively) [11,19,20,21,22].

Current estimates of genetic content on both Hsa21 and the homologous mouse regions put the number of genes at 552 and 436 genes respectively [12]. Of those genes, 166 are considered to be highly conserved (including the 5 microRNAs but excluding the

KRTAP genes), of which 162 have associated RefSeqP annotation [12]. There are an additional four RefSeqP genes that are mouse specific that are within the conserved syntenic regions. There are 274 non-RefSeqP genes in the mouse and 390 non-RefSeqP genes in the human that do not have apparent homology. Sturgeon and Gardiner [12] BLASTed the gene transcripts against the genomic region where the gene would be predicted to exist (based on neighboring genes that are conserved) and identified an additional 139 Hsa21 genes that have sequence conservation to regions of the mouse genome and 165 Mmu genes that have sequence conservation to regions of Hsa21 that are not represented in the list of 166 highly conserved genes [12]. This indicates that our parameters for determining highly conserved genes may be so strict that some conservation is being missed. These genes could have functional consequences that should be considered when looking at gene conservation.

Trisomic mouse models of DS

The large degree of conserved synteny supported the development of mouse models of DS. Multiple models have been developed, with varying amounts of trisomy of the regions that have conserved synteny with Hsa21. One of the first models was Ts16, in which the entire Mmu16 was trisomic due to a Robertsonian translocation [23]. This model had its limitations due to the fact that more than just the Hsa21 conserved regions were trisomic. The mice showed nervous system abnormalities that are similar to DS but the Ts16 pups were neonatal lethal, limiting their utility [24].

The most well studied model is Ts65Dn, a mouse model with a freely segregating chromosome consisting of a translocation between the centromeric portion of Mmu17 with the distal portion of Mmu16 (which contains the region that has conserved synteny with Hsa21 [7,23,25]). These mice are trisomic for 110 genes that are highly conserved with Hsa21 [26]. This model develops learning and memory deficits that are analogous to DS, as well as having a reduced cerebellum similar to individuals with DS [25,27]. In addition, the Ts65Dn mice develop craniofacial abnormalities that are analogous to the craniofacial features of DS [28].

There are other models with smaller segmental regions, Ts1Cje and Ts1Rhr, which contain fewer genes that are conserved with Hsa21, still within the Mmu16 conserved region. In these reduced trisomic models, the severity of the cerebellar phenotype varies based on the total trisomic content [29]. By using combinations of these models, we can narrow down regions of interest for different DS phenotypes.

Use of various mouse models with different amounts of trisomic gene content have been used to more precisely define contributions of different genetic segments to specific phenotypes [24,30], but even the smallest segmental trisomic mouse model still contains many genes. A few transgenic mouse models made for individual genes have been used to study the effects of gene dosage imbalance of single genes as they relate to DS [24], but these transgenic models are costly and time consuming to make and so have only been made for candidate genes that were suspected to have a large effect. The time,

effort and cost to make transgenic models for all the highly conserved genes on Hsa21 are prohibitive to using this approach in an unbiased manner.

Using zebrafish as a model system

The ability to study early developmental anomalies presents another limitation of mouse models. In order to study developmental stages in mice, a pregnant female has to be euthanized, and the embryos removed and fixed. Each stage requires a separate litter, increasing the cost and time if the intent is to look at multiple stages of development. There are now methods for ex-vivo imaging of mouse embryos, predominately for use in embryos 6-10 days post-coitum (dpc), but only for up to 24 hours of culturing, and these methods are very sensitive to environmental control (even small shifts in temperature can be detrimental) and still require fixing of the embryos after 12-24 hours of imaging and still don't have the necessary resolution [31,32]. The resolution of these techniques are still not enough for use in studying specific organs and tissues.

In contrast, zebrafish make an attractive model for studying early development. External fertilization and a large number of progeny allow for large scale screening of early development [33]. Most organ systems develop within the first 24 hours, and by 5 days post-fertilization (DPF) the embryos are free swimming [34]. The transparency of the zebrafish embryo adds to its utility, allowing for the visualization of tissue and organ development as a whole organism in real time, avoiding the necessity of fixing and sectioning in order to examine the internal structures as in mice [35]. This in turn allows for the ability to follow a single embryo throughout early development, making zebrafish

a powerful model system for studying the effects of Hsa21 gene expression during embryogenesis. Additionally, in zebrafish the craniofacial development parallels the development in higher vertebrates [36]. There are many transgenic reporter lines for specific cell types and tissues [34,37,38].

A major difficulty in understanding DS is that trisomy 21 originates prior to fertilization, with every cell trisomic for Hsa21, causing downstream effects throughout development. The trisomic genes could have an primary effect directly on the cellular function due to over-expression of a dosage sensitive gene, or could have a secondary effect on the expression and regulation of disomic genes that then have further downstream actions [27]. The ability to make distinctions between these possibilities would be useful when attempting to ameliorate the phenotypes in DS as correcting a single dosage sensitive gene would be potentially easier than correcting a pathway that must be carefully regulated. Since many aspects of DS develop during embryogenesis, zebrafish allow for the analysis of expression of Hsa21 genes during early development. To facilitate the development of genotype-phenotype correlations, I have used zebrafish as a model system to study the effects of over-expression of Hsa21 genes during early development.

CHAPTER 2: CREATION OF THE HUMAN CHROMOSOME 21 GENE EXPRESSION CLONE-SET

Introduction:

We sought to develop a Hsa21 gene expression clone-set that would be useful in both in vivo and in vitro studies. Our goal was to develop gene expression set that could be cloned into a vector system that was versatile and efficient, containing a set of genes from Hsa21 that, while not comprehensive of the total gene list, would comprise the majority of genes that might be of interest to the DS community.

The vector system we chose was the Invitrogen Gateway recombination system [39]. This vector system uses an entry vector plasmid containing attL sites on either side of restriction digest cloning sites. These sites can specifically recombine with attR sites located on destination vectors, allowing for easy and efficient sub-cloning of cDNAs from the entry vector into any number of destination vectors. The destination vectors contain a ccdB cassette that is toxic to most standard bacterial cells flanked by attR sites. Using LR clonase (an excisionase) along with an integrase from bacteriophage delta and an integration host factor, the attL sites recombine with the attR sites, resulting in the two plasmids: the expression plasmid that contains the ORF of interest flanked by attB sites and the former entry vector which contains the lethal ccdB cassette flanked by attP sites (so only the expression vector will propagate in standard bacterial cells).

The sub cloning can be performed in 96-well plates, making this system efficient for large gene sets. There are a number of destination vector systems that would be useful for

the DS community. Many destination vectors include tags at the 3' or 5' ends, as well as other modifications, and different promoters are available for expression in both cell culture plasmid vectors as well as vectors for use in zebrafish [35].

In this study we obtained or sub-cloned 169 Hsa21 genes (171 cDNAs, two genes are represented by two isoforms) into the Invitrogen Gateway recombination system, and then sub cloned into the pCS+ destination vector which contains both a CMV promoter for expression in mammalian cell culture as well as an SP6 promoter and SV-40 poly-A tail for use in vitro RNA transcription.

Methods:

Hsa21 Gene Expression Library preparation

Genes from Hsa21 included in the library were curated from lists of genes conserved between human and mouse [11,12]. For 120 genes, plasmids containing the gene in the pENTR222 entry vector were obtained through the Invitrogen Gateway ORFeome collection (Figure 1). The remaining 49 genes were sub cloned from a variety of vectors into one of the Invitrogen Gateway entry vectors (for complete list of original vectors and sources see Appendix 1, for list of primers used for TOPO cloning see Table 2). Clones were selected

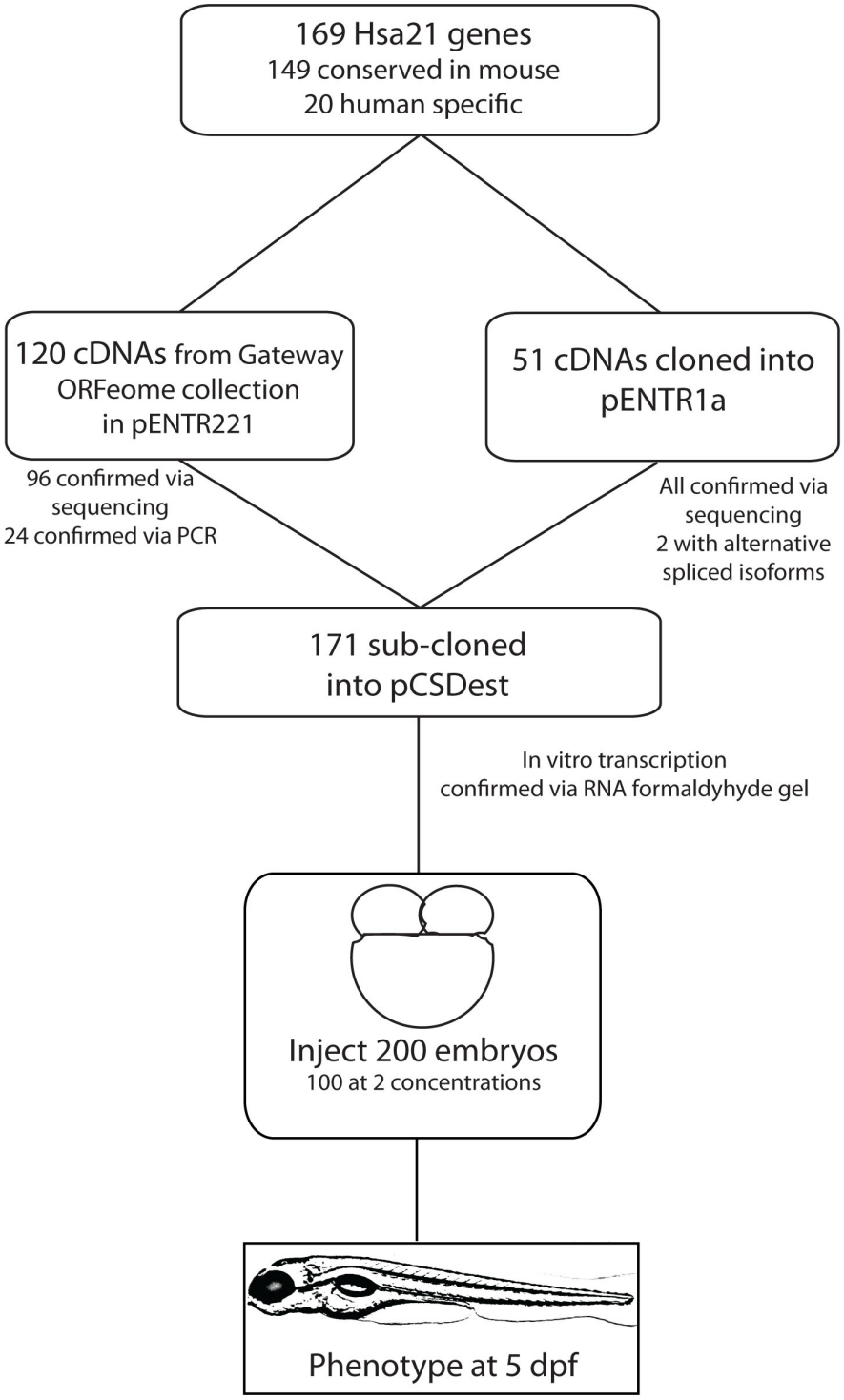

Figure 1: Flowchart showing steps of making the Hsa21 Gene Expression Clone-set and the screen of the set in zebrafish

Table 1: List of primers used for TOPO cloning

Gene Symbol	TOPO Forward Primer	TOPO Reverse Primer
B3GALT5	CACCATGGCTTTCCC GAAGATGAGATTG	TCAGACAGGCGGACA ATCTTC
BACH1	CACCATGTCTCTGAG TGAGAACTCG	TGCAAGTTTACTCAT CAGTAGTACATTTATC
Col6a1	CACCATGAGGGCGGC CCGTGCTCTGC	CTAGCCCAGCGCCAC CTTCCTG
DOPEY2	CACCATGGTGACAGT CCCTCCCATTGCT	TCAGACACCATGATG GGCCAC
DSCAM	CACCATGTGGATACT GGCTCTCTCCTT	GAGCTCGAATTCGTT TAAACTACCAGGGTGTAAG
DSCR10	CACCATGCAGATTGT GCAGGGGTTC	TCACACAGGCATACA CACGG
DYRK1A	CACCATGCATACAGG AGGAGAGACTTCA	CTATTACGAGCTAGC TACAGGACTCTGTT
ITSN1	CACCATGGCTCAGTT TCCAACACCT	CTACGGCTCATCAAA CAACTG
LCA5L	CACCATGTCTTTGGC TGATCTAAC	AAACCAGAATGCATT AGGATATTGA
LRRC3	CACCATGGGCACCGT GCGCCCACCTCG	CTAGGGCCCCGGGCC GATGGGG
MCM3AP long	CACCATGAACCCAAC TAATCCTTTCAGTG	GCTCAAATGTCCACC ATGTCT
MRPL39	CACCATGGAGGCGCT GGCCATGGGTTCC	TTAGGTAGATGTACA TTCCTC
PLAC4	CACCATGGGGACAAC AAGGAGTATCC	TCAGGACTGGGGGAC TGAAGAGAC
SIM2	CACCATGAAGGAGAA GTCCAAGAATG	AAGCCCTACTTAGAA GCAGAAAGAG
SYNJ1-145	CACCATGGCGTTCAG TAAAGGATTC	CCTGTTACCCTGATG GTTGC
SYNJ1-170	CACCATGGCGTTCAG TAAAGGATTC	GCGTTATCTTTCTGT AAAGTCCAGTG
TRPM2	CACCATGGAGCCCTC AGCCCTGAGG	TCAGTAGTGAGCCCC GAAC
TTC3	CACCATGGACAATTT TGCTGAG	TGACTACCTAGAAGA GCAGGAAG
USP25	CACCATGACCGTGGA GCAGAACGTGC	GCACGTTCTGCTCCA CGGTCAT

using kanamycin and then sequenced to confirm presence of gene. All genes in the entry vector were then sub-cloned into the pCS2Des vector (Invitrogen) using LR clonase as previously described [39]. Genes in the pCS2+ vector were selected for by ampicillin. The pCS2+ vector clone set, named the Hsa21 Gene Expression Set, is available for purchase through AddGene.

Results/Discussion

Development of the clone-set

We assembled a set of Hsa21 cDNA clones consisting of 169 Hsa21 genes, 149 that are highly conserved between human and mouse and 20 human specific genes [11,12]. Two genes, *SYNJ1* and *MCM3AP*, were each represented by two isoforms for a total of 171 cDNAs (Appendix 1). Cloning into the Invitrogen Gateway™ entry vector allows efficient sub-cloning of large sets of genes into destination vectors suitable for many experimental designs such as transcription, mammalian expression and the addition of tags. The pCS2+ vector contains an SP6 promoter that supports transcription of RNA and a CMV promoter for expression of transfected plasmid in mammalian cells and tissues.

Genes included in clone-set

Predominately, this study set consists of genes that are conserved in mice. Of the 169 genes included, 147 were curated from lists of conserved genes from Gardiner and colleagues [11,12]. Seventeen of the remaining genes are on Sturgeon and Gardiner's list of Hsa21 genes that are considered to have associated RefSeq proteins but are not

conserved [12], of which eleven are found in a list of human specific genes [11]. Six genes are included in the clone-set that are not in Sturgeon and Gardiner's list of genes on Hsa21, but are listed in the NCBI database as being on Hsa21 (*TPTE, TMPRSS3, BAGE, BAGE4, C21ORF37*, and *C21ORF125*; accessed April 15, 2013 [40]). *TPTE* was found to be conserved in position but minimally conserved in sequence with mouse *Tpte* (BLAST with 76% sequence identity over 55% coverage through the mRNA). *TMPRSS3* was found to be highly conserved with mouse *Tmprss3*, with 86% identity over 60% of the mRNA. *BAGE* and *BAGE4* are two members of the B melanoma antigen family, with no conservation in mouse. Lastly, there are two ORFs, *C21ORF37* and *C21ORF125*, which have been classified as non-coding RNA.

Of the 164 genes considered to be highly conserved with mouse, 17 genes are not included in our screen. Five of those genes are microRNAs, which have to be specifically processed for proper function, and it was determined that our assay in fish would not allow for proper processing, additionally the 3' untranslated region is not expected to have the degree of sequence conservation necessary for proper microRNA function. One gene is listed as unknown gene type in the NCBI database with no RefSeq protein associated (which was listed in Sturgeon and Gardiner 2011 as having a RefSeq protein). Some of the genes had large coding regions that made cloning difficult, e.g. *SON*. And others of the genes were ORFs that were difficult to obtain.

This set of Hsa21 genes should prove to be a useful tool for the DS community. The ability to efficiently and quickly sub-clone the set into other destination vectors allows

for flexibility in a research paradigm, such that modifying genes with fluorescent tags can be done in a high throughput manner [35,39]. Additionally, destination vectors have been developed with different promoters, including a CMV promoter for eukaryotic expression, an SP6 promoter for prokaryotic expression, as well as promoters for tissue/cell specific expression [35]. Vectors continue to be developed, meaning that this system, and this clone-set, will be useful for many different research labs.

CHAPTER 3: SCREENING THE HSA21 CLONE-SET IN ZEBRAFISH

Introduction

Interest in genotype-phenotype correlations has been ongoing among the DS community for decades, both using human patients as well as animal model systems. In humans, individuals with partial trisomy 21 along with detailed phenotyping was used to attempt to narrow down the region of Hsa21 that might be critically involved in either DS as a whole, or in specific phenotypes of DS (e.g. CHD, AMKL, cognitive impairment or craniofacial features, [14,15,16,17,18]). In many cases either it was not possible to accurately distinguish a critical region, or the critical region described is large enough to contain many genes that would all then need to be carefully and systematically examined, or multiple susceptibility regions were found [16,18]. The establishment of genotype-phenotype correlations in humans is complicated by the lack of large enough sample sizes [14], not having enough patients with some of the specific phenotypes of interest, or in some cases the partial trisomy was part of larger complex genomic rearrangements that would complicate the analysis [17]. The genetic heterogeneity inherent in humans also complicates analysis, particularly of phenotypes that have variable penetrance and severity.

The many mouse models that have different trisomic segments that correspond to Hsa21 allow for potentially a more precise genotype-phenotype correlation since it's possible to obtain large enough sample sizes, and due to the inbred nature of mice there is less genetic heterogeneity masking trisomic effects [24,29]. But even with mice, there are limitations to their use in genotype-phenotype correlations. The use of mice with

successively smaller trisomic regions can be used to narrow a region, but phenotypes may be due to multiple non-contiguous genes and spatial-temporal expression of those genes could affect the presentation of the phenotype. Transgenic models of single Hsa21 genes can be used to examine the effects of single gene over-expression on the phenotype to narrow down causative genes, or genes that may play a role in many DS phenotypes [41]. These transgenic models are costly and time intensive to make and assess, inhibiting their use in a high throughput unbiased manner.

Zebrafish are a valuable model to examine early development. The large number of progeny allow for the use of hundreds of embryos per experiment, and the short generation time (most structures are formed by 5 DFP [34]) make zebrafish an ideal system for a large genetic screen. I used the Hsa21 Gene Expression clone-set to examine the effects of expression of individual Hsa21 genes on early development by injecting the mRNA into zebrafish embryos and screening for phenotypes at 5 DPF.

Methods

In vitro transcription of mRNA

Plasmids containing genes from Hsa21 were transcribed in vitro using the mMessage mMachine SP6 kit. Plasmids were linearized with the appropriate restriction enzyme (see Appendix 2 and Figure 1), then purified by precipitation. Genes were transcribed with mMessage mMachine SP6 polymerase then treated with DNAse1. mRNA was purified with lithium chloride. mRNA quality and quantity was confirmed with a formaldehyde agarose gel and the Nanodrop8000 respectively.

Zebrafish maintenance and injections

Zebrafish were raised in the FINZ center at the Institute for Genetic Medicine (Johns Hopkins University) as previously described [42]. Zebrafish were maintained at 28°C. Male and female Tubingen zebrafish were placed in the same breeding tank in the morning and embryos were collected 30 minutes later. One hundred embryos were then injected at the 1-4 cell blastulae stage using a Ziess Stemi 2000 microscope and PV820 Pneumatic picopump injector. For each gene, there were two concentrations of mRNA injected: 10pg and 50pg or 50pg and 100pg. A cut off of 10% penetrance was used for all phenotypes except for rare phenotypes that are not observed in controls, e.g. cyclopia and craniofacial abnormalities. All candidates were re-injected at 100pg. Embryos were raised to 5 days post fertilization and then phenotyped using a Nikon SMZ1500 microscope and imaged with NIS Elements Imaging Software. After imaging, embryos were fixed in 4% PFA overnight then transferred to 100% methanol for storage at -20°C.

Morpholino rescue

Translation inhibiting antisense morpholinos (MO) were designed against the human sequence for the genes SOD1, RWDD2B, and CCT8, designed to bind to the ATG start codon of the mRNA using Gene Tools (Philomath, OR): SOD1 5'-GCACGCACACGGCCTTCGTCGCCAT-3'; RWDD2B 5'-GCTGCATGGACAGCTCAATTTTCAT-3'; and CCT8 5'-GAGCCTTGGGAACGTGAAGCGCCAT-3'. The MOs were checked using BLAST to ensure sequence specificity to the human homologue and that they did not match any

other sequence in the human or zebrafish genome. For JAM2, the MO used was designed against the zebrafish homologue, Jam2a, as previously described [43]. For each gene, 100 embryos were injected with 2ng MO, 100 embryos were injected with 100pg of mRNA and 100 embryos were injected with both 2ng MO and 100pg mRNA. Also, 100 un-injected embryos were used as a control. Embryos were examined at 5 dpf for SOD1 and RWDD2B, 4 dpf for CCT8, and 24 hpf for JAM2. The embryos were assayed at the earliest stage at which the phenotype was most easily identified.

Histogram

All plates were examined for the presence of any abnormal fish, and a penetrance (% of total embryos) was calculated for each plate independently. Penetrances were grouped in a histogram, with the y-axis representing the number of plates that had a specific penetrance of abnormal fish. Non-candidates were plotted separately from candidates. An average penetrance was calculated for the non-candidates, the twenty-three and ten candidates. The candidates (ten and twenty-three) were compared to the non-candidates using a Student t-test for significance.

Statistical Tests

For the morpholino rescue experiment and the combinatorial injections, penetrance differences were examined using a Fisher's Exact test with a $p < 0.05$ required for significance. For the histogram data, Student T-tests were used to compare the non-candidates average penetrance to the twenty-three candidates and ten candidates

Results

Zebrafish screen

RNAs were synthesized from 171 Hsa21 cDNA clones and each was injected into one hundred 1-2 cell zebrafish embryos at each of two concentrations (either 10pg and 50pg, or 50pg and 100pg, see Appendix 2). The embryos were allowed to develop through 5 DPF and screened for gross morphological changes. We compared the frequency of a given defect in injected fish compared to controls. Observed phenotypes included U-shaped somites and cyclopia, both of which are associated with defects in the Shh pathway and the ciliome; craniofacial abnormalities and pigment differences, which may be related to aberrations of neural crest cells; and pericardial edema (Figure 2). In every case, the phenotype was incompletely penetrant, i.e., fewer than 100% of the embryos were affected. A wide range of penetrance was observed for different genes, and in independent injection cohorts with the same gene.

Of the 171 RNAs, twenty-three showed a phenotype after the initial screen, including fourteen that gave a Shh/ciliome - related phenotype (eight with U-shaped somites and six with cyclopia), seven with phenotypes related to neural crest cells (four with craniofacial abnormalities and three with pigment differences), one gene that resulted in a pericardial edema phenotype and one that produced a fin phenotype (Appendix 2 and Table 2). Fresh RNA was prepared from these first round candidates and the injections were repeated.

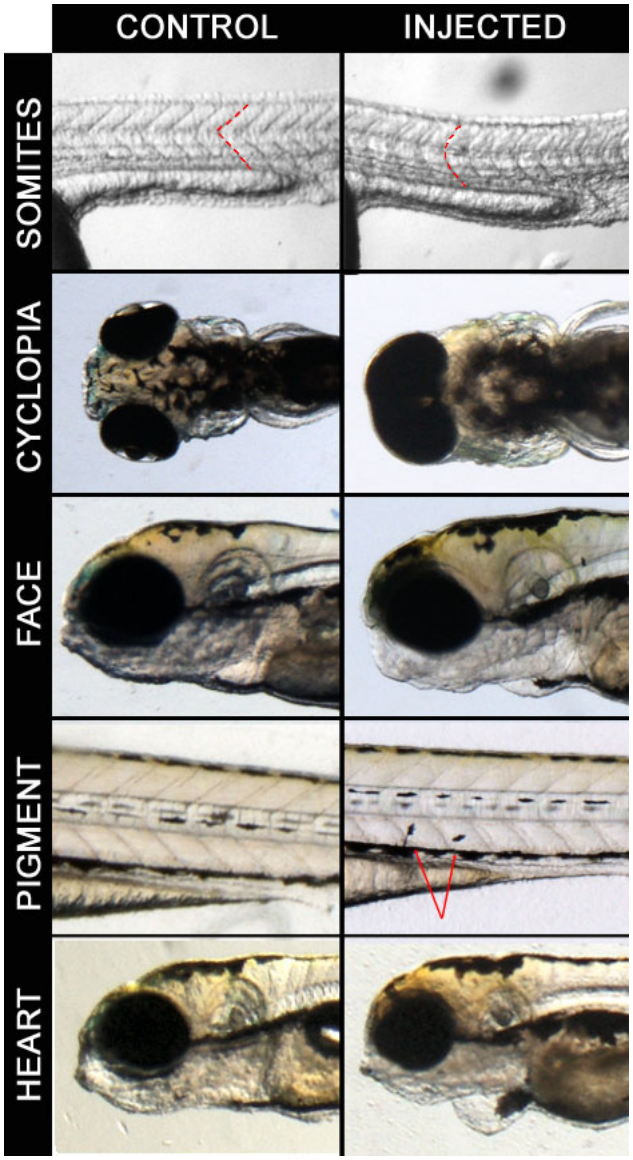

Figure 2: Examples of phenotypes observed in screen. Control embryos are on the left panel and injected embryos are on the right panel. Somites: *RWDD2B* 100pg injected embryos at 24 hpf with dashed lines to highlight somitic boundaries. Cyclopia: *C21ORF84* 100pg injected embryos at 5 dpf. Pigment: *CCT8* 100pg injected embryos at 4 dpf, arrows indicating melanocytes. Heart: *JAM2* 100pg injected embryos at 48 hpf.

Table 2: Twenty-three candidates from first pass of screen

Phenotype category	Description	# Candidates
U-shaped Somites	Somites with characteristic U shape	8
Cyclopia	Single large eye	6
Craniofacial abnormalities	Small/missing mandible; skull abnormalities	4
Pigment abnormalities	Floating melanocytes; reduced pigment in eye	3
Heart	Pericardial edema	1
Other	Tail/fin abnormalities	1

Ten candidates robustly recapitulated the original phenotypes; seven from the Shh/ciliome groups, two with neural crest related phenotypes, and the gene resulting in pericardial edema (Figure 2 and Table 3).

Phenotypic rescue via Morpholinos

We performed a morpholino (MO) rescue experiment with four candidate genes to determine whether the phenotypes observed are due to the expression of the specific RNA and not to RNA toxicity. Translation-blocking MOs were designed against the human copies of *SOD1*, *RWDD2B* or *CCT8* and against the zebrafish orthologues of *JAM2*. One hundred embryos were injected with just RNA, just MO, and RNA +MO. For all four genes, injection of the RNA alone produced significantly higher penetrance than the uninjected controls, the MO alone or the MO+RNA injected embryos ($p<0.05$; Figure 3). For *SOD1*, *RWDD2B*, and *CCT8,* the MO+RNA was not significantly different from the controls. *JAM2* MO+RNA showed heart edema significantly more frequently than controls, but was significantly less than the RNA alone.

Dosage and gene expression patterns

All ten candidates were injected at three or more concentrations ranging from 10pg to 200pg but no linear correlation between dosage and penetrance was observed (Figure 4).

Table 3: Final candidate list of genes that recapitulated the phenotype after re-injection.

Gene Symbol	Phenotype	Penetrance	Expression in mouse [44]
SOD1	U-somites	10-35%	Expressed ubiquitously at E10.5, strongly expressed in muscles at E14.5
RWDD2B	U-somites	15-31%	Expressed ubiquitously at E10.5
RRP1	U-somites	15-40%	Weakly expressed in somites at E10.5 [45]
PCBP3	U-somites	8-13%	Expressed in brain and spinal cord at E14.5
YBEY	U-somites	12-19%	Expressed ubiquitously at E10.5
C21orf84	U-somites/ Cyclopia	9-23% U-somites 0-7% cyclopia	human specific [11]
POFUT2	Cyclopia	0-4%	Strong in face and pharyngeal arches at E9.5 [45]
CBR3	Craniofacial	7-10%	Expressed ubiquitously at E10.5, strong in cartilage at E14.5
CCT8	Pigment	15-40%	Expressed ubiquitously at E10.5
JAM2	Pericardial Edema	20-60%	High expression in human heart [46]

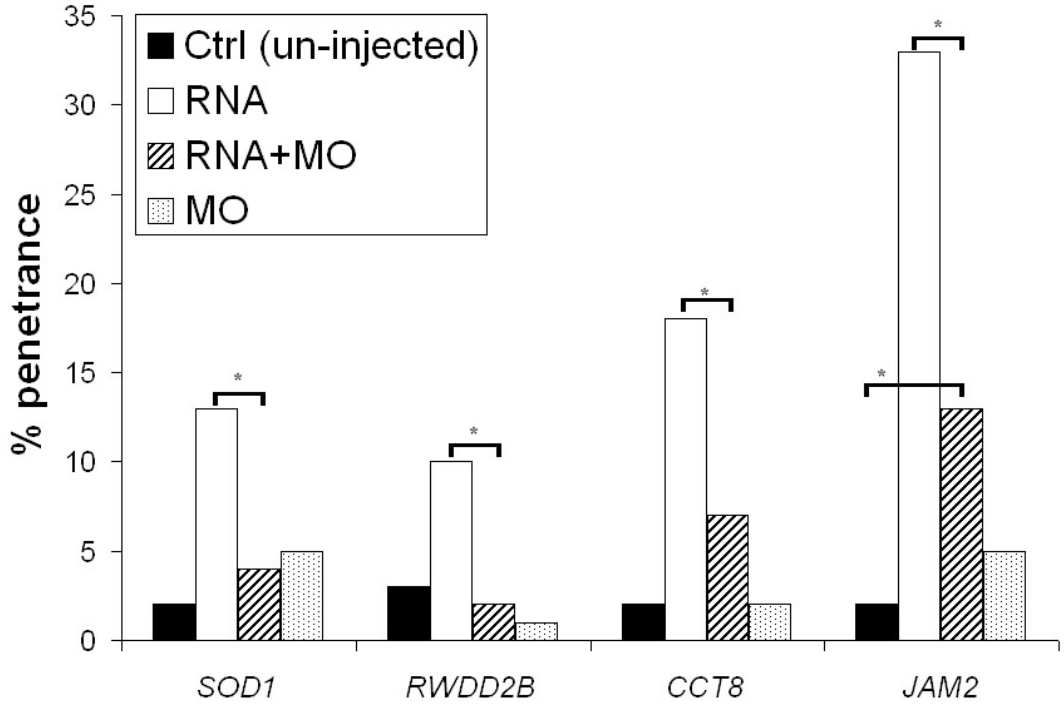

Figure 3: Four of the 10 candidates (SOD1, RWDD2B, CCT8, and JAM2) were co-injected with translational blocking morpholino. 100pg RNA was injected alone, 2 ng MO alone, or both were co-injected, using un-injected embryos as a control. * Fisher's Exact Test p-value <0.05

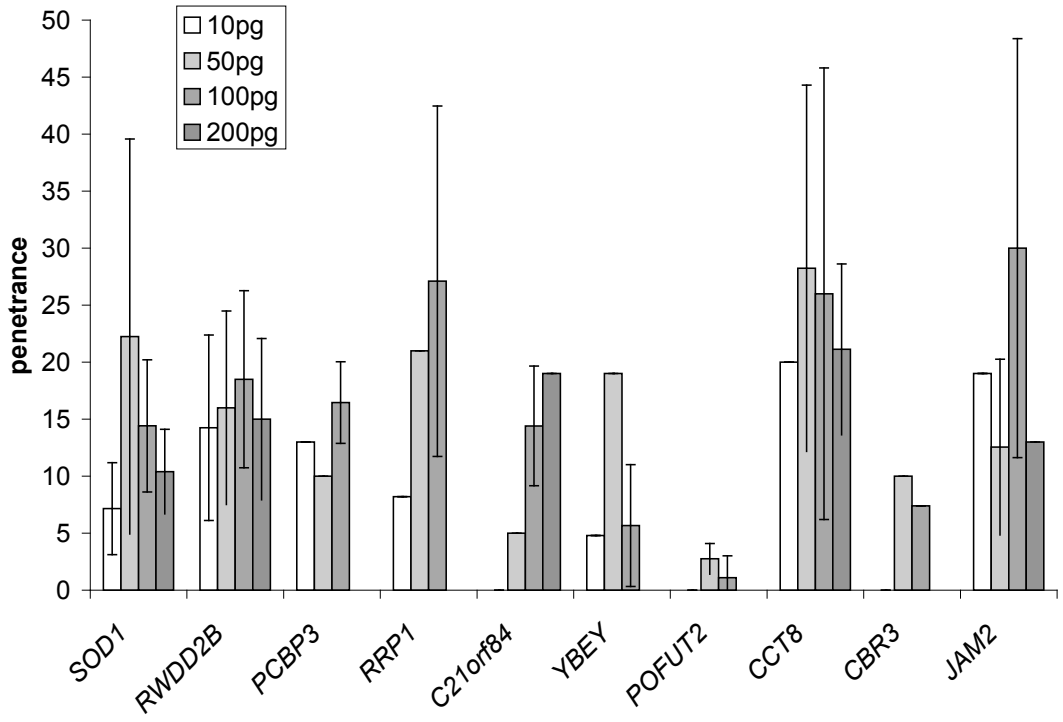

Figure 4: Penetrance of phenotypes of candidate genes at different dosages.

Eight of the ten candidates have zebrafish homologues, the exceptions being *C21ORF84* and *CBR3*. Seven of those eight genes have representative *in situ* hybridization data available in the ZFIN catalog. For most of the candidates, the gene was shown to be expressed in the structure affected by RNA injection. *Sod1*, *Rrp1*, *Ybey* are expressed in somites; *Cct8* is expressed ubiquitously; and *Jam2* shows expression in the region of the developing heart (Table 3). *Pofut2* is expressed in the brain and eye, which is consistent with its cyclopia phenotype. However, *Pcbp3*, which caused U-shaped somites, is not detectable by *in situ* hybridization in early development and *Rwdd2b* was not present in the ZFIN catalog. Nine of the ten candidates have mouse orthologues whose expression has been examined at mid-gestation, and in each case, the genes are expressed in the corresponding locations during embryonic development in mouse (Table 3, [44,45]). *C21ORF84* is human specific, but shows homology with primate [11].

Histogram of phenotypic data

Some phenotypes, e.g. U-shaped somites and edema, are found frequently at low penetrance in many injections as well as in the control embryos. Other phenotypes such as cyclopia and craniofacial abnormalities occur rarely in injected embryos and never in control embryos. To understand the distributions penetrance of the more common phenotypes, the frequency of observing abnormal embryos was evaluated for non-candidate genes and candidate genes separately, the spread of the penetrance of abnormalities examined. All injected embryos were examined for any abnormal embryos and the penetrance of abnormality was determined both for embryos that were injected with genes that did not cause phenotypes as well as for embryos injected with the

candidate genes. The number of plates of embryos that had a particular penetrance was visualized as the frequency in a histogram (Figure 5).

Penetrance of abnormality among the non-candidates was examined from 281 plates of injected embryos, and averaged to 9.57% abnormal. All 175 injected plates from the twenty-three candidates was also examined for all abnormalities and prepared in a similar histogram, with an average of 16.3% abnormal embryos (t-test, p= 7.1E-10 compared to non-candidates). The ten final candidates were examined separately from the thirteen candidates that did not replicate and of those 125 plates, there was an average of 17.2% abnormal embryos (t-test, p=6.57E-09 compared to non-candidates). The candidate genes clearly have a right shift in distribution of penetrance compared to the non- candidates. These data suggests that our cut off of 10% for most of the phenotypes (excluding the rare phenotypes, such as cyclopia) was sufficient to account for the presence of general abnormalities within the embryo population.

Discussion:

We have conducted the first large-scale study of the effects of Hsa21 expression on early embryogenesis. Previous analyses of Hsa21 gene expression in early development used *in situ* hybridization [44,47] or microarrays to examine the localization, timing and levels of Hsa21 gene up-regulation [48]. In this study we used a functional assay in zebrafish to find candidate genes with effects on early development in a systematic approach. This stage of development is difficult to study in other vertebrates. Ten genes were implicated in affecting the ciliome/Shh signaling, NCC or the heart. Several of the genes found

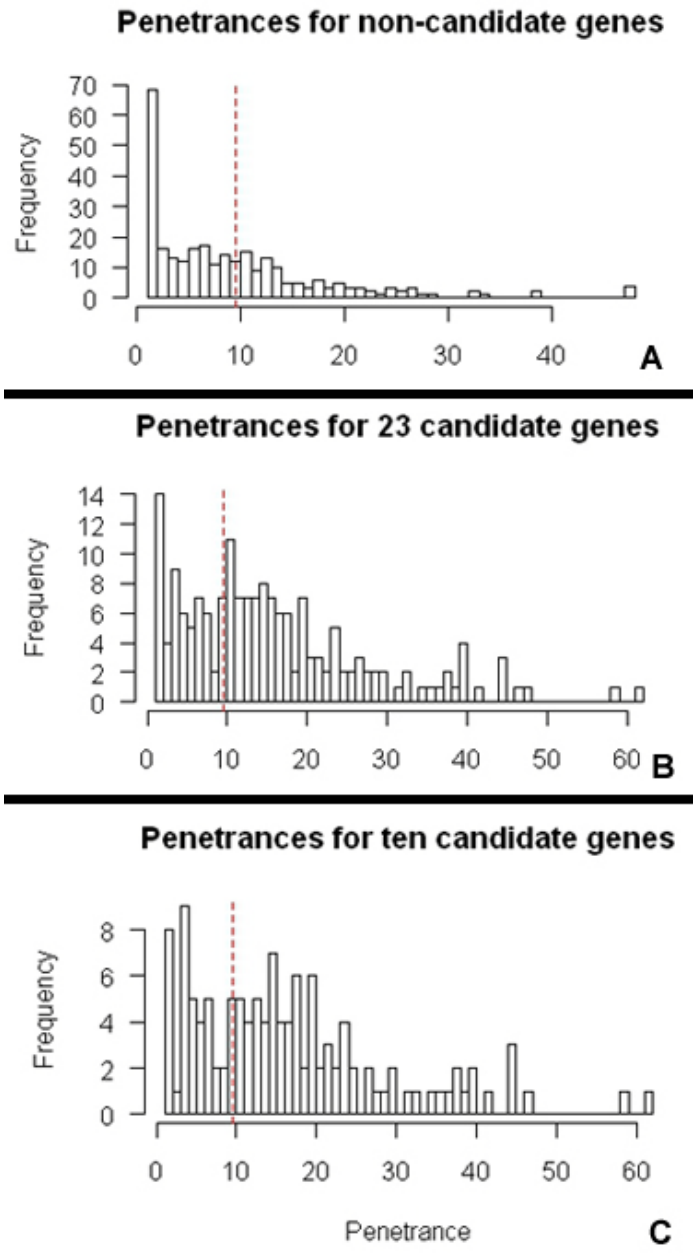

Figure 5: Histogram of frequency of observed penetrance of abnormalities from zebrafish screen. A. the 148 genes in which no observable phenotype was determined. B. Twenty-three candidates from the first pass of the screen. C. The ten final candidates. Red dashed line represents the average penetrance of the non-candidate genes for comparison to the candidates.

through this screen have little or no known function, and none have a known role in either the ciliome/Shh signaling pathway or NCC generation and development.

In this screen we identified ten genes that are candidates for further study. *CCT8* and *CBR3* are associated with pigment abnormalities and craniofacial abnormalities, respectively, which suggests a role in the proliferation, migration or differentiation of NCC. *CCT8* encodes a chaperonin that is localized to the cytoplasm [49], and has a potential role in histone modification due to its association with histone deacetylase C3 (HDAC3 [50]). *CBR3* is a carbonyl reductase gene, for which there is little information about function. (Although it is similar structurally to CBR1, the two genes likely have different substrates [51]). Neither of these genes are currently associated with regulation of NCC. *JAM2*-injected embryos had a repeatable and robust pericardial edema phenotype, indicating a possible role in heart development, which is further supported by evidence in the mouse that it is expressed in fetal and adult heart, and may be involved in cardiac inflammatory conditions [46]. There's evidence that *JAM2* is involved in lymphocyte adhesion [52], so it's possible that it facilitates edema through the immune pathway instead of affecting the development of the heart.

Three of the genes identified in the screen (*RWDD2B*, *YBEY* and *C21ORF84*) have very little known information and no known function. *RWDD2B* has been identified in a handful of large protein-protein interaction screens, with possible interactions with DDX19 [53], as well as a possible substrate for SRPK2, a serine/arginine protein kinase [54]. There is no information about *C21ORF84*, other than that it is described as a long

intergenic non-coding RNA. In a yeast-two hybrid screen, Ybey was shown to have a protein-protein interaction with Gem, a GTP binding protein expressed in skeletal muscle [55]. These three genes, along with *PCBP3*, *POFUT2* and *RRP1* were found to have either U-shaped somites or cyclopia. *RRP1* is involved in the processing of rRNA [56]. *PCBP3* binds to C-rich pyrimidine regions of RNA, but no known established function has been shown, although it was a hypothesized role in post-transcriptional regulation [57]. *POFUT2* is an O-fucosyltransferase, whose target protein substrates are components of the extra-cellular matrix [58]. *SOD1* is another candidate for a possible Shh related phenotype due to its U-shaped somite phenotype. Transgenic *SOD1* mice had impaired muscle function as assessed by the rope grip test [59]. *SOD1* is not known to play a role in Shh signaling, but it is expressed at the neuromuscular junction, which may indicate that it acts upstream of the Shh pathway [60,61]. In fact evidence suggests that mutations in Sod1 in mice (G93A, a common mutation used for the study of Amyotrophic lateral sclerosis) result in altered morphology of slow twitch and fast twitch muscle fibers, with the slow twitch fibers should a great variation in muscle fiber diameter with an over all shift towards smaller fibers in both slow twitch and fast twitch [62]. This could be analogous to the U-shaped somite phenotype in the zebrafish, which suggests that the effect of *SOD1* on the U-shaped somite phenotype is related to its effect on the neuromuscular junction.

A negative result in the screen does not rule out contribution of that gene to DS. Some mRNAS might have been inefficiently translated due to the fact that these are human mRNAs in fish. Some human proteins may simply be unrecognizable to the fish, e.g., a

growth factor requires a specific receptor to function. Nonetheless, it was somewhat surprising that several Hsa21 genes that have been associated with dramatic phenotypes in mouse models of DS did not produce a phenotype in this screen. For example, *DSCAM*, a cell adhesion molecule that is involved in cell recognition [63] and has been implicated in both heart and neurogenesis defects in DS [64] but did not produce a phenotype here. *DYRK1A*, a dual specificity kinase expressed during early neurogenesis that has been the subject of pilot trials for treatment of cognitive deficits in DS [65,66,67], also produced no phenotype in our screen. While these negative results were surprising, many types of refined screens with greater sensitivity and specificity are possible, taking advantage of transgenically marked zebrafish lines to ask specific questions about development of specific cells and tissues.

Negative results in the screen could also result from stoichiometric issues. Results from the different dosages of the ten final candidate genes did not show a significant difference in penetrance due to dosage, suggesting that the system is being saturated; and these concentrations are similar to other studies [68,69]. However, there is still the possibility that genes that gave negative results at 10pg and 50pg may in fact have shown a response at 100pg or more. And in fact, some genes (notably transcription factors) have been reported anecdotally to produce phenotypes at very low concentrations that are not present when much more mRNA is injected; there is not currently a robust explanation for such a phenomenon.

Although this screen is purely observational, these data provide evidence for possible roles in the Shh pathway, NCC regulation and the heart. Further characterization of these candidates could provide functional information for genes, some of which have no functions described. In a more candidate based approach, these genes would likely have been missed.

CHAPTER 4: PAIR-WISE COMBINATORIAL INJECTIONS OF SHH RELATED CANDIDATE GENES

Introduction

As previous studies have shown, there are multiple regions of Hsa21 that are responsible for the many DS features, indicating that many features result from dosage imbalance of more than one gene [7,13,24,27]. These genes individually may have small or no effect, but together can have a larger effect on one or more developmentally important pathways [27,70]. A benefit of the zebrafish model is that this possibility can be evaluated in a pair-wise fashion in a manner that is more technically difficult in mice. To evaluate this, I performed pair-wise injections of Hsa21 genes to evaluate their ability to cause a phenotype in combination. To perform pair-wise injections of 171 cDNAs would require >14,000 injections, which was not feasible. Instead I focused on the largest group of candidates from the screen: genes that gave a Shh related phenotype of either U-shaped somites or cyclopia.

In the somites, the Shh pathway activates *myf5* which regulates myogenesis [71]. Shh is required for myogenesis maintenance and controls the cell fate decision between fast muscle and slow muscle. Absence of Shh leads to loss of slow muscle fibers and the level of Shh signaling affects the induction of muscle pioneer cells within the slow muscle fibers, with higher levels of signaling required for muscle pioneer cells than for the non-pioneer slow muscle [72]. Changes in level of Shh activation affect the differentiation of the different classes of muscle fibers, leading to the loss of the muscle

pioneer cell and increased fast muscle fibers, which in turn causes the somites to become U-shaped.

In zebrafish, there are a number of mutant lines that are called "you-type" mutations due to the presence of U-shaped somites [73]. Many of the you-type mutations were found to occur in genes that are part of the Shh pathway. For example, sonic you, *syu*, was determined to be a mutation in *shh-a*; you-too, *yot*, is a mutation in *gli2*; slow muscle omitted, *smu*, is a mutation in *smo*, [73,74]). Additionally, when either of the two zebrafish orthologues for *SHH*, *shh-a* and *shh-b*, are knocked down using MO, the embryos exhibit U-somites and when both are knocked-down the fish developed cyclopia, as well [75]. This indicates that the presence of U-shaped somites or cyclopia might reflect abnormal regulation of the Shh pathway. Of the ten final candidates, seven gave phenotypes relating to the Shh pathway. These genes had either U-shaped somites and/or cyclopia.

To look for possible additive effects of over-expression, the seven genes giving Shh-related phenotypes were injected in a pair-wise fashion, using *C21ORF84* as the reference gene that was co-injected with the other six genes. *C21ORF84* was the only gene that had both cyclopia and U-somites.

Methods:

Pair-wise injections:

RNA from *C21ORF84* was co-injected with RNA from the following genes: *SOD1*, *RWDD2B*, *RRP1*, *PCBP3*, *POFUT2*, and *YBEY*. For each experiment, each gene was injected individually at 100pg into 100 embryos, and then co-injected at 100pg of each RNA for a total of 200pg RNA. Uninjected embryos were used as controls. Embryos were phenotyped at 24 hpf for the presence of U shaped somites and cyclopia. Each co-injection was performed twice.

Combinatorial Injections:

Plasmids containing *DSCAM*, *SH3BGR*, *DCSR6*, *ADAMTS1*, *COL6A1*, *COL6A2*, and *Col18A1* were transcribed in vitro as previously described. For *SH3BGR*, *DCSR6*, and *ADAMTS1*, 30 pg of each mRNA were combined for a total of 90 pg, injected into 100 zebrafish embryos, and then examined for phenotypes at 5 DPF. For *DSCAM* and *SH3BGR*, 50 pg each were combined for a total of 100pg RNA injected into 100 embryos and phenotyped at 5 DPF. For *COL6A1*, *COL6A2*, and *Col18A1*, 50 pg each were combined for a total of 150pg of RNA injected into 100 embryos and phenotyped 5 DPF.

Statistical Tests

Penetrance differences were examined using a Fisher's Exact test with a $p < 0.05$ required for significance.

Results:

We first examined the seven genes with Shh/ciliome phenotypes. For each set of pair-wise injections, *C21ORF84* was injected alone at 100pg, the second gene was injected

alone at 100pg, and both genes were injected together at 100pg each. Injection of *C21ORF84* plus *YBEY*, *PCBP3* or *POFUT2* showed a significant increase in penetrance of U-shaped somites (Fig. 6, $p<0.05$ for each combination). For two genes, *SOD1* and *RWDD2B*, there was no significant difference between the individual injections and the combinatorial injection. *RRP1* alone had a penetrance of 42%, the highest of all the genes. This frequency was significantly reduced in embryos injected with *RRP1* and *C21ORF84*.

We also assessed candidate gene sets for possible combinatorial effects on developmental phenotypes. Co-injection of *SH3BGR*, *DCSR6* and *ADAMTS1* (30pg each), produced cyclopia in 3.6% and peri-cardial edema in a non-overlapping 3.6% of fish, whereas no control embryos were observed to have either edema or cyclopia, a strong trend though not formally significant (Fisher's exact test, $p=0.056$ for either cyclopia or edema). Several Hsa21 gene combinations have been implicated in the high frequency of congenital heart disease in DS [46]. However, neither injection of all three collagens together (*COL6A1, COL6A2, Col18A1*) nor co-injection of *DSCAM* and *SH3BGR* produced a significant frequency of heart (or other) defects.

Discussion:

When using mouse models of DS, a subtractive approach is usually used, in which a phenotype is examined in the model with the largest trisomic content, and then continuing to use progressively smaller trisomic models until the phenotype is no longer observed. Once a list of possible candidate genes is found, knock-out mice of the

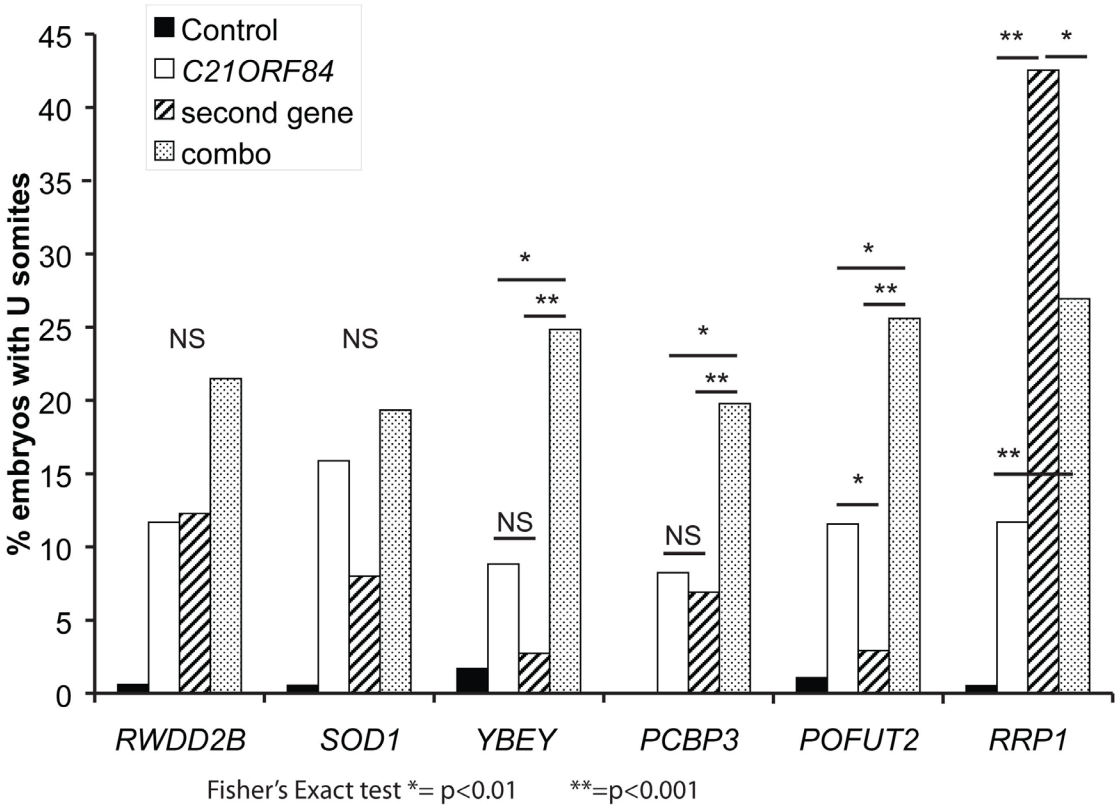

Figure 6: Pair-wise combinatorial injections of Shh candidate genes. *C21ORF84* was co-injected with 6 other genes to look for synthetic effects. *C21ORF84* was injected individually at 100pg RNA, the other gene was injected individually at 100pg RNA and then the two were injected together, 100pg each, for a total of 200pg RNA

candidates can be crossed with the trisomic mice and examined for absence of the phenotype [23]. In our study I chose an additive approach, starting with single genes that produced a phenotype and then performing pair-wise combinatorial injections using genes that gave related phenotypes. I observed that some of the genes can interact in an additive manner, some have no apparent interaction and one pair had a compensatory interaction. The compensatory interaction in which *RRP1* and *C21ORF84* together had lower penetrance than *RRP1* alone supports the idea that it is the totality of the different effects of the many genes from Hsa21 that can cause a particular effect or phenotype. These pair-wise interactions could be expanded to include more combinations, including co-injecting genes that have similar proposed function or genes that are suspected to interact with each other (candidate based). These could also be repeated in marked fish to narrow in on specific phenotypes.

Compensatory interaction implies that over-expression of one gene in this pathological condition can balance the increased expression of another. Clearly the universe of possible individual gene effects and interactions in DS is large. The system described here provides an effective way to interrogate more complex interactions of non-contiguous genes from the earliest stages of development.

CHAPTER 5. CONCLUDING REMARKS

Many outcomes of trisomy 21 might result from perturbations of a limited number of pathways that are "common denominators" of multiple phenotypes [70]. An example is the Sonic hedgehog pathway (Shh) which has been shown to be down-regulated in the brains of mouse models of DS [76]. This results in cerebellar hypoplasia and hypo-cellularity, which can be rescued by stimulation with SAG, a Shh agonist [76]. The attenuated response to Shh in Ts65Dn may also contribute to the craniofacial abnormalities resulting from the reduced proliferation and migration of neural crest cells (NCC) from the first pharyngeal arch in the developing mouse embryo [77]. Since Shh signaling is important in many aspects of prenatal development, down regulation of the pathway could result in defects in many tissues, including the brain, craniofacial skeleton, and heart, all of which are affected in individuals with DS [70].

In the canonical Shh pathway, Shh binds to its receptor Patched (Ptc), which releases its repression on Smoothened (Smo), which moves into the cilium [78,79,80]. There, Smo triggers the degradation of Suppressor of Fused (Sufu), which relieves Sufu's binding of the Gli2 and Gli3 transcription factors, preventing them from being protealytically cleaved into their repressor forms. This leaves them in their activated form where they then move to the nucleus and act as transcription factors for down stream targets, including Gli1 and Ptc, as well as genes involved in cell cycle regulation [70,80].

Non-canonical Shh pathway activation can involve different components of the Shh pathway but with different down stream effects. For example, Ptc can inhibit cyclin B1

translocation independent of Smo, affecting proliferation; independently Ptc can undergo caspase cleavage and induce apoptosis [79]. Shh can also act outside the Ptc-Smo-Gli pathway, possibly affecting NCC migration in a Smo-independent fashion. Smo also has non-canonical activities, with recent research suggesting that it can act outside of the cilia, and that in fact its localization affects its activity; when localized to the cilia, Smo acts via the canonical pathway through Gli-mediated transcription, but when localized outside the cilium, Smo can affect a chemotactic response [81]. It's possible that the maintenance of the correct ratio of Smo to either the cilium or other cellular locales is essential for proper development.

Until recently there were no genes on Hsa21 that were known to play a direct role in the Shh pathway. Evidence suggests that a cleavage product of *APP* may play a role in regulating the SHH receptor, *PTCH* [82].

In zebrafish, the process of somitogenesis begins shortly after gastrulation with the segmentation of the paraxial mesoderm that flanks the notochord into blocks of cells of uniform size [73]. This process involves the action of the somite clock which involves oscillations of the *notch* pathway, along with *her1* and *her4* genes that regulate the timing of the segmentation, while opposing gradients of FGF/Wnt and retinoic acid regulate the position of segmentation [73,83]. The pre-somitic mesoderm (PSM) undergoes mesenchymal-epithelial transition, and the somites become mesenchyme surrounded by an epithelial layer, after which the somites are morphologically distinct [73,84]. The PSM then differentiates into sclerotome and myotome, eventually becoming the axial

skeleton and muscle. The myotome differentiates from there into three classes of muscle fibers: fast muscle fibers that form deep in the core of the somites, while non-pioneer slow muscle fiber develop on the surface of the myotome and pioneer slow muscle (distinguished by the expression of Engrailed) differentiates adjacent to the notochord [73]. It is the careful balance of many developmental factors and pathways that regulate the differentiation of the myotome into their different fast and slow fibers. Genes that affect this process of somitogenesis could alter the development of the somites, causing a morphological change, such as the U-shaped somites observed in this screen.

Due to a partial genome duplication event approximately 250 million years ago, some human genes have multiple zebrafish orthologues [34]. This is the case for SHH. The zebrafish orthologues of SHH, *shh-a* and *shh-b*, are expressed in the notochord and floor plate and are a mitogen for somitic cells [85]. Among the you-type mutation strains, the U-somite phenotype in the *syu* embryos is milder than that observed in the *yot* and *smu*, which suggests that *shh-b* can compensate for *shh-a* [73]. When both *shh-a* and *shh-b* are knocked down with MOs, not only does the penetrance of the U-somites increase, but the embryos also begin to develop cyclopia [75].

It is possible that the candidate genes that had U-shaped somites may affect the Shh pathway in a way that disrupts its induction of slow muscle fibers, resulting in the U-somites. These genes could be playing a role in the regulation or maintenance of the Shh pathway. If they are involved in the Shh pathway during somitogenesis, they may also act in the pathway during other developmental events during embryogenesis. Over

expression of these genes may be involved in the Shh pathway down regulation observed in the cerebellum and craniofacial development in mice.

The additive effects observed in the pair-wise injections suggest that some of the Shh candidate genes may act in concert on the Shh pathway. The genes not showing an additive effect may be affecting the pathway in ways that are independent of each other, or some of the genes could be acting outside of the canonical pathway. Additionally, there is always the possibility that the genes are affecting the shape and development of the somites independently from Shh. An example is the case of the choker mutant zebrafish (*cho*) where evidence suggest that, although these embryos develop U-somites and are considered to be a you-type, they also develop melanophore abnormalities which are attributed to the defect in somite development which likely occurs downstream of the Shh induced differentiation of the slow muscle fibers [86]. Although the six genes that gave U-shaped somite phenotype may be affecting the Shh pathway, it is also possible that they are causing the U-shaped somites independent of the Shh pathway. These genes should be explored further to rule out that possibility and confirm whether they have an effect on the Shh pathway.

The Hsa21 Gene Expression clone-set described here will be a useful tool for the DS community. Screening the clone-set in zebrafish produced a number of candidates with robust and replicable phenotypes with implications for effect on the Shh pathway, NCC, and heart development. The Shh-related genes showed signs of additive effects in a pair-wise set of injections, showing that this system can be used to study both the individual

effects of Hsa21 gene expression as well as combinatorial effects of multiple gene expression. This study can be expanded upon by repeating the screen in transgenic zebrafish models as well as expanding upon the combinatorial injections using a candidate based approach as well as more unbiased methods.

Appendix 1: 169 genes/171 cDNAs in Hsa21 clone-set

Gene Name	Zebrafish Plate/Well	Gene Start (bp)	Accession #
ABCG1	P2/H3	43619799	NM_004915
ADAMTS1	P1/B4	28208606	BC036515
ADAMTS5	P1/C4	28290231	BC093777
ADARB1	P2/F8	46493768	NM_015833
AGPAT3	P2/E6	45285067	BC004219
AIRE	P2/A7	45705721	BC103511
ANKRD20A11P	P1/E1	15316090	Q8NFU9
ANKRD30BP2	P1/C1	14410487	AF427490
APP	P1/H3	27252861	NM_000484
ATP5J	P1/F3	27088815	NM_001003696
ATP5O	P1/B9	35275757	NM_001697
B3GALT5	P2/G1	40928369	BC104864
BACE2	P2/D2	42539728	NM_012105
BACH1	P1/C5	30566392	BC063307
BAGE	P1/B1	11057796	NM_001187
BAGE4	P1/D1	14741931	NM_181704
BRWD1	P2/B1	40556102	NM_001007246
BTG3	P1/G2	18965971	NM_001130914
C21orf119	P1/E6	33765439	NR_026845
C21orf125	P2/G5	44869904	Q6ZR72
C21orf128	P2/G3	43522244	BC063412
C21orf2	P2/C7	45748827	NM_001271441
C21orf37	P1/E2	18811208	NR_037585
C21orf49	P1/E7	34144411	AK096601
C21orf59	P1/A7	33951132	NM_021254
C21orf67	P2/B8	46352729	AY035381
C21orf77	P1/G6	33944548	BC027970
C21orf88	P2/H1	40969074	BC119737
C21orf91	P1/H2	19161284	BC015468
C2CD2	P2/D3	43305221	BC062323
CBR1	P1/D10	37442239	NM_001757
CBR3	P1/E10	37507210	NM_001236
CBS	P2/C5	44473301	NM_000071
CCT8	P1/A5	30428126	BC005220
CHAF1B	P1/G10	37757676	NM_005441
CHODL	P1/A3	19165801	NM_024944
CLDN14	P1/H10	37832919	NM_012130

Appendix 1: 169 genes/171 cDNAs in Hsa21 clone-set

Gene Name	Zebrafish Plate/Well	Gene Start (bp)	Accession #
CLDN17	P1/E5	31538241	NM_012131
CLDN8	P1/F5	31586324	NM_199328
CLIC6	P1/A10	36041688	BC075706
Col18a1	P2/E8	46825052	NM_001109991
Col6a1	P2/A9	47401651	BC052575
COL6A2	P2/B9	47518011	BC002484
CRYAA	P2/E5	44589118	NM_000394
CRYZL1	P1/H8	34961647	NM_145858
CSTB	P2/C6	45192393	NM_000100
CXADR	P1/F2	18884700	NM_001338
CYYR1	P1/A4	27838528	BC036761
DIP2A	P2/A10	47878812	NM_001146115
DNAJC28	P1/E8	34860238	BC029509
DNMT3L	P2/H6	45666222	BC002560
DONSON	P1/G8	34947783	BC043316
DOPEY2	P1/F10	37529080	BC057081
DSCAM	P2/C2	41382926	AB384859
DSCR10	P1/F12	39578250	BC093855
DSCR3	P1/H11	38591910	BC110655
DSCR4	P1/C12	39323728	NM_005867
DSCR8	P1/D12	39493545	AA707621
DSCR9	P1/G11	38580804	BC029827
DYRK1A	P1/A12	38739236	BC156309
ERG	P1/G12	39751949	NM_182918
ETS2	P1/H12	40177231	NM_005239
EVA1C	P1/F6	33784314	BC038710
FAM207A	P2/C8	46359955	NM_058190
FAM3B	P2/F2	42676139	NM_058186
FTCD	P2/C9	47556176	BC052248
GABPA	P2/A6	27106881	BC035031
GART	P1/F8	34870940	NM_175085
GRIK1	P1/D5	30909254	BC031822
HLCS	P1/B11	38123493	NM_000411
HMGN1	P2/C1	40714241	NM_004965
HSF2BP	P1/G3	44949072	NM_007031
HSPA13	P1/H1	15743436	BC036370

Appendix 1: 169 genes/171 cDNAs in Hsa21 clone-set

Gene Name	Zebrafish Plate/Well	Gene Start (bp)	Accession #
HUNK	P1/B6	33245628	NM_014586
IFNAR1	P1/B8	34696734	NM_000629
IFNAR2	P1/H7	34602206	BC002793
IFNGR2	P1/C8	34757299	NM_005534
IGSF5	P2/A2	41117334	BC004806
IL10RB	P1/A8	34638663	NM_000628
ITGB2	P2/A8	46305868	BC005861
ITSN1	P1/A9	35014706	BC116186
JAM2	P1/E3	27011584	NM_021219
KCNE1	P1/G9	35818988	BC036452
KCNE2	P1/E9	35736323	BC112087
KCNJ15	P1/E12	39529128	NM_002243
KCNJ6	P1/B12	38996789	NM_002240
LCA5L	P2/E1	40777770	BC031059
LINC00313 (C21orf84)	P2/H5	44881974	P59037
LINC00314 (C21orf94)	P1/D4	29385682	P59092
LINC00478 (C21orf34)	P1/D2	17442842	AA451643
LIPI	P1/F1	15481134	NM_198996
LRRC3	P2/E7	45875369	BC119648
LSS	P2/E9	47608360	BC035638
LTN1	P1/F4	30300466	BC150284
MAP3K7CL	P1/B5	30449792	BC008567
MCM3AP 3'	P2/G9	47655047	BC013285
MCM3AP long	P2/F9	47655047	BC104960
MIS18A	P1/C6	33640530	NM_018944
MRAP	P1/D6	33664124	NM_178817
MRPL39	P1/D3	26957968	BC107719
MRPS6	P1/C9	35445524	NM_032476
MX1	P2/H2	42792231	NM_001144925
MX2	P2/G2	42733870	BC035293
N6AMT1	P1/E4	30244513	BC011554
NCAM2	P1/C3	22370633	NM_004540
NDUFV3	P2/A5	44299754	NM_001001503
NRIP1	P1/B2	16333556	BC040361
OLIG1	P1/G7	34442450	NM_138983
OLIG2	P1/F7	34398153	BC036245

Appendix 1: 169 genes/171 cDNAs in Hsa21 clone-set

Gene Name	Zebrafish Plate/Well	Gene Start (bp)	Accession #
PAXBP1	P1/D7	34106210	BC030539
PCBP3	P2/H8	47063608	BC012061
PCP4	P2/B2	41239243	NM_006198
PDE9A	P2/G4	44073746	NM_001001567
PDXK	P2/B6	45138975	BC005825
PFKL	P2/B7	45719934	NM_002626
PIGP	P1/D11	38435146	NM_153681
PKNOX1	P2/B5	44394620	NM_004571
PLAC4	P2/E2	42547158	BC093685
POFUT2	P2/D8	46683843	NM_133635
PRDM15	P2/C3	43218385	BC067102
PRMT2	P2/C10	48055079	BC000727
PSMG1	P2/A1	40546695	NM_003720
PTTG1IP	P2/H7	46269500	NM_004339
PWP2	P2/G6	45527176	BC013309
RBM11	P1/G1	15588451	NM_144770
RCAN1	P1/H9	35885440	BC002864
RIPK4	P2/B3	43159529	BC110617
RIPPLY3	P1/C11	38378450	NM_018962
RRP1	P2/D6	45209394	NM_003683
RSPH1	P2/E4	43892596	BC101519
RUNX1	P1/B10	36160098	BC069929
RWDD2B	P1/G4	30378080	NM_016940
S100B	P2/B10	48018875	NM_006272
SAMSN1	P1/A2	15857549	NM_022136
SCAF4	P1/A6	33043313	NM_020706
SETD4	P1/C10	37406839	NM_001007259
SH3BGR	P2/F1	40817781	NM_001001713
SIK1	P2/F5	44834395	BC038504
SIM2	P1/A11	38071433	NM_005069
SLC19A1	P2/G8	46913486	BC003068
SLC37A1	P2/F4	43916128	NM_018964
SLC5A3	P1/D9	35445870	NM_006933
SMIM11	P1/F9	35747749	NM_058182
SOD1	P1/H5	33031935	NM_000454
SPATC1L	P2/D9	47581062	NM_032261

Appendix 1: 169 genes/171 cDNAs in Hsa21 clone-set

Gene Name	Zebrafish Plate/Well	Gene Start (bp)	Accession #
SUMO3	P2/G7	46191374	NM_006936
SYNJ1-145	P1/B7	33997269	AF009039
SYNJ1-170	P1/C7	33997269	NM_003895
TCP10L	P1/H6	33948862	NM_144659
TFF1	P2/C4	43782391	NM_003225
TFF2	P2/B4	43766466	NM_005423
TFF3	P2/A4	43731777	BC017859
TIAM1	P1/G5	32361860	BC117196
TMEM50B	P1/D8	34804792	NM_006134
TMPRSS15	P1/B3	19641433	BC111749
TMPRSS2	P2/A3	42836478	NM_005656
TMPRSS3	P1/E11	38437942	NM_032405
TPTE	P1/A1	10906201	BC028719
TRAPPC10	P2/F6	45432206	AB001517
TRPM2	P2/D7	45770046	BC112342
TTC3	P1/F11	38445571	BC137345
U2AF1	P2/D5	44513066	NM_006758
UBASH3A	P2/D4	43824008	BC028138
UBE2G2	P2/F7	46188955	NM_182688.2
USP16	P1/H4	30396950	BC030777
USP25	P1/C2	17102344	BC075792
WDR4	P2/H4	44263204	NM_018669
WRB	P2/D1	40752170	NM_004627
YBEY	P2/H9	47706267	NM_001006114
ZNF295	P2/E3	43406940	BC063290
ZNF295-AS1	P2/F3	43442113	Q8N0V1

Appendix 1: 169 genes/171 cDNAs in Hsa21 clone-set continued

Gene Name	Catalog # *	Original vector
ABCG1	IOH52605	pENTR221
ADAMTS1	IOH22476	pENTR221
ADAMTS5	OP#7939622	pCR4-TOPO
ADARB1	IOH38242	pENTR221
AGPAT3	IOH5155	pENTR221
AIRE	OP#40039054	pCR-BluntII-TOPO
ANKRD20A11P	IOH43458	pENTR221
ANKRD30BP2	IOH50106	pENTR221
APP	IOH5590	pENTR221
ATP5J	IOH4502	pENTR221
ATP5O	IOH13236	pENTR221
B3GALT5	OP#8143867	pCR4-TOPO
BACE2	IOH13508	pENTR221
BACH1	OP#MHS1010-9204253	pBluescriptR
BAGE	IOH50070	pENTR221
BAGE4	IOH50065	pENTR221
BRWD1	IOH39941	pENTR221
BTG3	IOH10468	pENTR221
C21orf119	IOH6691	pENTR221
C21orf125	IOH35140	pENTR221
C21orf128	OP#5207414	pCMV-SPORT6
C21orf2	IOH23207	pENTR221
C21orf37	IOH50121	pENTR221
C21orf49	IOH50135	pENTR221
C21orf59	IOH4573	pENTR221
C21orf67	OP#40022796	pCR-BluntII-TOPO
C21orf77	IOH11976	pENTR221
C21orf88	OP#40119171	pCR-BluntII-TOPO
C21orf91	IOH11236	pENTR221
C2CD2	IOH40678	pENTR221
CBR1	IOH3944	pENTR221
CBR3	IOH5424	pENTR221

* Invitrogen Gateway ORFeome clones begin with IOH; Open Biosystems clones begin with OP

Appendix 1: 169 genes/171 cDNAs in Hsa21 clone-set

Gene Name	Catalog # *	Original vector
CBS	IOH10211	pENTR221
CCT8	IOH7383	pENTR221
CHAF1B	IOH13577	pENTR221
CHODL	IOH12081	pENTR221
CLDN14	IOH12590	pENTR221
CLDN17	IOH35308	pENTR221
CLDN8	IOH12281	pENTR221
CLIC6	OP#2648653	pCMV-SPORT6
Col18a1	Harvard MmCD00319800	pCMV-SPORT6.1
Col6a1	OP#6598940	pOTB7
COL6A2	IOH4285	pENTR221
CRYAA	IOH40243	pENTR221
CRYZL1	IOH22501	pENTR221
CSTB	IOH2908	pENTR221
CXADR	IOH10207	pENTR221
CYYR1	OP#MHS1010-7508527	pCMV-SPORT6
DIP2A	IOH21776	pENTR221
DNAJC28	IOH22569	pENTR221
DNMT3L	IOH4002	pENTR221
DONSON	OP#5320969	pCMV-SPORT6
DOPEY2	OP#5704600	pYX-Asc
DSCAM	Kazusa#FXC00331	pFK1
DSCR10	OP#7939700	pCR4-TOPO
DSCR3	OP#6157155	pCMV-SPORT6
DSCR4	IOH40378	pENTR221
DSCR8	IOH13220	pENTR221
DSCR9	IOH28674	pENTR221
DYRK1A	OP#100061742	pENTR223.1
ERG	IOH26275	pENTR221
ETS2	IOH10422	pENTR221
EVA1C	IOH26808	pENTR221
FAM207A	IOH13437	pENTR221
FAM3B	IOH29166	pENTR221

* Invitrogen Gateway ORFeome clones begin with IOH; Open Biosystems clones begin with OP

Appendix 1: 169 genes/171 cDNAs in Hsa21 clone-set

Gene Name	Catalog # *	Original vector
FTCD	OP#6270063	pOTB7
GABPA	IOH27140	pENTR221
GART	IOH26153	pENTR221
GRIK1	OP#4501004	pCMV-SPORT6
HLCS	IOH29186	pENTR221
HMGN1	IOH4772	pENTR221
HSF2BP	IOH2965	pENTR221
HSPA13	IOH22345	pENTR221
HUNK	Harvard HsCD00399347	pENTR223.1
IFNAR1	IOH56150	pENTR221
IFNAR2	IOH5316	pENTR221
IFNGR2	IOH3856	pENTR221
IGSF5	OP#3584645	pCMV-SPORT6
IL10RB	IOH4959	pENTR221
ITGB2	IOH6210	pENTR221
ITSN1	OP#40073781	pCR-BluntII-TOPO
JAM2	OP#MHS6278-202840811	pDNR-LIB
KCNE1	IOH22480	pENTR221
KCNE2	OP#8327555	pCR4-TOPO
KCNJ15	IOH13007	pENTR221
KCNJ6	IOH42392	pENTR221
LCA5L	OP#5271223	pBluescriptR
LINC00313 (C21orf84)	IOH34931	pENTR221
LINC00314 (C21orf94)	IOH43062	pENTR221
LINC00478 (C21orf34)	IOH50122	pENTR221
LIPI	HsCD00080183 from DNASU	pENTR223.1
LRRC3	OP#40115796	pCR-BluntII-TOPO
LSS	OP#5547173	pCMV-SPORT6
LTN1	OP#8860138	pBluescriptIISK+
MAP3K7CL	IOH3328	pENTR221
MCM3AP 3'	OP#MHS1011-75220	pOTB7
MCM3AP long	OP# MHS4426-99240373	pCR-XL-TOPO
MIS18A	IOH28068	pENTR221

* Invitrogen Gateway ORFeome clones begin with IOH; Open Biosystems clones begin with OP

Appendix 1: 169 genes/171 cDNAs in Hsa21 clone-set

Gene Name	Catalog # *	Original vector
MRAP	IOH40717	pENTR221
MRPL39	OP#MHS1011-98053826	pDNR-LIB
MRPS6	IOH13845	pENTR221
MX1	IOH21990	pENTR221
MX2	OP#5182160	pCMV-SPORT6
N6AMT1	IOH12718	pENTR221
NCAM2	IOH28826	pENTR221
NDUFV3	IOH21750	pENTR221
NRIP1	IOH25775	pENTR221
OLIG1	IOH26795	pENTR221
OLIG2	IOH62196	pENTR221
PAXBP1	IOH21633	pENTR221
PCBP3	IOH12489	pENTR221
PCP4	IOH22123	pENTR221
PDE9A	IOH9807	pENTR221
PDXK	IOH5866	pENTR221
PFKL	IOH6888	pENTR221
PIGP	IOH44755	pENTR221
PKNOX1	IOH6384	pENTR221
PLAC4	OP#7939530	pCR4-TOPO
POFUT2	IOH39914	pENTR221
PRDM15	IOH62935	pENTR221
PRMT2	IOH4698	pENTR221
PSMG1	IOH3819	pENTR221
PTTG1IP	IOH10419	pENTR221
PWP2	IOH5155	pENTR221
RBM11	IOH22581	pENTR221
RCAN1	IOH5722	pENTR221
RIPK4	OP#40034395	pCR-BluntII-TOPO
RIPPLY3	IOH35236	pENTR221
RRP1	IOH3452	pENTR221
RSPH1	OP#8069025	pCR4-TOPO

* Invitrogen Gateway ORFeome clones begin with IOH; Open Biosystems clones begin with OP

Appendix 1: 169 genes/171 cDNAs in Hsa21 clone-set

Gene Name	Catalog # *	Original vector
RUNX1	OP#4008335	pCMV-SPORT6
RWDD2B	IOH12821	pENTR221
S100B	IOH4935	pENTR221
SAMSN1	IOH22118	pENTR221
SCAF4	IOH57303	pENTR221
SETD4	IOH5697	pENTR221
SH3BGR	IOH45822	pENTR221
SIK1	IOH29894	pENTR221
SIM2	Harvard HsCD00346299	pCR-BluntII-TOPO
SLC19A1	IOH4768	pENTR221
SLC37A1	IOH37911	pENTR221
SLC5A3	IOH36106	pENTR221
SMIM11	IOH29335	pENTR221
SOD1	IOH4089	pENTR221
SPATC1L	IOH14034	pENTR221
SUMO3	IOH4668	pENTR221
SYNJ1-145	Addgene 22291	pcDNA3-FLAG
SYNJ1-170	Addgene 22292	pcDNA3-FLAG
TCP10L	IOH21795	pENTR221
TFF1	IOH21839	pENTR221
TFF2	IOH21844	pENTR221
TFF3	IOH13105	pENTR221
TIAM1	OP#40125747	pCR-XL-TOPO
TMEM50B	IOH4187	pENTR221
TMPRSS15	IOH36299	pENTR221
TMPRSS2	IOH27076	pENTR221
TMPRSS3	IOH35575	pENTR221
TPTE	IOH11625	pENTR221
TRAPPC10	IOH28065	pENTR221
TRPM2	OP#40069893	pCR-BluntII-TOPO
TTC3	HsCD00342640 (Harvard)	pCR-XL-topo
U2AF1	IOH4817	pENTR221
UBASH3A	IOH11540	pENTR221
UBE2G2	IOH45834	pENTR221
USP16	IOH22293	pENTR221

* Invitrogen Gateway ORFeome clones begin with IOH; Open Biosystems clones begin with OP

Appendix 1: 169 genes/171 cDNAs in Hsa21 clone-set

Gene Name	Catalog # *	Original vector
USP25	OP#30346400	pBluescriptR
WDR4	IOH6391	pENTR221
WRB	IOH10553	pENTR221
YBEY	IOH58675	pENTR221
ZNF295	Harvard MMCD00346299	pCMV-Sport6
ZNF295-AS1	IOH21603	pENTR221

* Invitrogen Gateway ORFeome clones begin with IOH; Open Biosystems clones begin with OP

Appendix 1: 169 genes/171 cDNAs in Hsa21 clone-set continued

Gene Name	cloning method	entry vector
ABCG1	NA	pENTR221
ADAMTS1	NA	pENTR221
ADAMTS5	RD cloning	pENTR1a
ADARB1	NA	pENTR221
AGPAT3	NA	pENTR221
AIRE	RD cloning	pENTR1a
ANKRD20A11P	NA	pENTR221
ANKRD30BP2	NA	pENTR221
APP	NA	pENTR221
ATP5J	NA	pENTR221
ATP5O	NA	pENTR221
B3GALT5	TOPO cloning	pENTR-Dtopo
BACE2	NA	pENTR221
BACH1	TOPO cloning	pENTR-Dtopo
BAGE	NA	pENTR221
BAGE4	NA	pENTR221
BRWD1	NA	pENTR221
BTG3	NA	pENTR221
C21orf119	NA	pENTR221
C21orf125	NA	pENTR221
C21orf128	RD cloning	pENTR1A
C21orf2	NA	pENTR221
C21orf37	NA	pENTR221
C21orf49	NA	pENTR221
C21orf59	NA	pENTR221
C21orf67	RD cloning	pENTR1A
C21orf77	NA	pENTR221
C21orf88	RD cloning	pENTR1A
C21orf91	NA	pENTR221
C2CD2	NA	pENTR221
CBR1	NA	pENTR221
CBR3	NA	pENTR221
CBS	NA	pENTR221
CCT8	NA	pENTR221
CHAF1B	NA	pENTR221
CHODL	NA	pENTR221

Appendix 1: 169 genes/171 cDNAs in Hsa21 clone-set continued

Gene Name	cloning method	entry vector
CLDN14	NA	pENTR221
CLDN17	NA	pENTR221
CLDN8	NA	pENTR221
CLIC6	BP clonase	pDONOR221
Col18a1	BP clonase	pENTR223.1
Col6a1	TOPO cloning	pENTR-Dtopo
COL6A2	NA	pENTR221
CRYAA	NA	pENTR221
CRYZL1	NA	pENTR221
CSTB	NA	pENTR221
CXADR	NA	pENTR221
CYYR1	BP clonase	pDONOR221
DIP2A	NA	pENTR221
DNAJC28	NA	pENTR221
DNMT3L	NA	pENTR221
DONSON	BP clonase	pDONOR221
DOPEY2	TOPO cloning	pENTR-Dtopo
DSCAM	TOPO cloning	pENTR-Dtopo
DSCR10	TOPO cloning	pENTR-Dtopo
DSCR3	BP clonase	pDONOR221
DSCR4	NA	pENTR221
DSCR8	NA	pENTR221
DSCR9	NA	pENTR221
DYRK1A	TOPO cloning	pENTR-Dtopo
ERG	NA	pENTR221
ETS2	NA	pENTR221
EVA1C	NA	pENTR221
FAM207A	NA	pENTR221
FAM3B	NA	pENTR221
FTCD	BP clonase	pDONOR221
GABPA	NA	pENTR221
GART	NA	pENTR221
GRIK1	BP clonase	pDONOR221
HLCS	NA	pENTR221

Appendix 1: 169 genes/171 cDNAs in Hsa21 clone-set continued

Gene Name	cloning method	entry vector
HMGN1	NA	pENTR221
HSF2BP	NA	pENTR221
HSPA13	NA	pENTR221
HUNK	NA	pENTR223.1
IFNAR1	NA	pENTR221
IFNAR2	NA	pENTR221
IFNGR2	NA	pENTR221
IGSF5	BP clonase	pDONOR221
IL10RB	NA	pENTR221
ITGB2	NA	pENTR221
ITSN1	TOPO cloning	pENTR-Dtopo
JAM2	RD cloning	pENTR221
KCNE1	NA	pENTR221
KCNE2	RD cloning	pENTR1A
KCNJ15	NA	pENTR221
KCNJ6	NA	pENTR221
LCA5L	TOPO cloning	pENTR-Dtopo
LINC00313 (C21orf84)	NA	pENTR221
LINC00314 (C21orf94)	NA	pENTR221
LINC00478 (C21orf34)	NA	pENTR221
LIPI	NA	pENTR223.1
LRRC3	TOPO cloning	pENTR-Dtopo
LSS	BP clonase	pDONOR221
LTN1	RD cloning	pENTR1a
MAP3K7CL	NA	pENTR221
MCM3AP 3'	BP clonase	pDONOR221
MCM3AP long	TOPO cloning	pENTR-Dtopo
MIS18A	NA	pENTR221
MRAP	NA	pENTR221
MRPL39	TOPO cloning	pENTR-Dtopo
MRPS6	NA	pENTR221
MX1	NA	pENTR221
MX2	BP clonase	pDONOR221
N6AMT1	NA	pENTR221

Appendix 1: 169 genes/171 cDNAs in Hsa21 clone-set continued

Gene Name	cloning method	entry vector
NCAM2	NA	pENTR221
NDUFV3	NA	pENTR221
NRIP1	NA	pENTR221
OLIG1	NA	pENTR221
OLIG2	NA	pENTR221
PAXBP1	NA	pENTR221
PCBP3	NA	pENTR221
PCP4	NA	pENTR221
PDE9A	NA	pENTR221
PDXK	NA	pENTR221
PFKL	NA	pENTR221
PIGP	NA	pENTR221
PKNOX1	NA	pENTR221
PLAC4	TOPO cloning	pENTR-Dtopo
POFUT2	NA	pENTR221
PRDM15	NA	pENTR221
PRMT2	NA	pENTR221
PSMG1	NA	pENTR221
PTTG1IP	NA	pENTR221
PWP2	NA	pENTR221
RBM11	NA	pENTR221
RCAN1	NA	pENTR221
RIPK4	RD cloning	pENTR1a
RIPPLY3	NA	pENTR221
RRP1	NA	pENTR221
RSPH1	RD cloning	pENTR1A
RUNX1	BP clonase	pDONOR221
RWDD2B	NA	pENTR221
S100B	NA	pENTR221
SAMSN1	NA	pENTR221
SCAF4	NA	pENTR221
SETD4	NA	pENTR221
SH3BGR	NA	pENTR221
SIK1	NA	pENTR221

Appendix 1: 169 genes/171 cDNAs in Hsa21 clone-set continued

Gene Name	cloning method	entry vector
SIM2	TOPO cloning	pENTR-Dtopo
SLC19A1	NA	pENTR221
SLC37A1	NA	pENTR221
SLC5A3	NA	pENTR221
SMIM11	NA	pENTR221
SOD1	NA	pENTR221
SPATC1L	NA	pENTR221
SUMO3	NA	pENTR221
SYNJ1-145	TOPO cloning	pENTR-Dtopo
SYNJ1-170	TOPO cloning	pENTR-Dtopo
TCP10L	NA	pENTR221
TFF1	NA	pENTR221
TFF2	NA	pENTR221
TFF3	NA	pENTR221
TIAM1	RD cloning	pENTR1a
TMEM50B	NA	pENTR221
TMPRSS15	NA	pENTR221
TMPRSS2	NA	pENTR221
TMPRSS3	NA	pENTR221
TPTE	NA	pENTR221
TRAPPC10	NA	pENTR221
TRPM2	TOPO cloning	pENTR-Dtopo
TTC3	TOPO cloning	pENTR-Dtopo
U2AF1	NA	pENTR221
UBASH3A	NA	pENTR221
UBE2G2	NA	pENTR221
USP16	NA	pENTR221
USP25	TOPO cloning	pENTR-Dtopo
WDR4	NA	pENTR221
WRB	NA	pENTR221
YBEY	NA	pENTR221
ZNF295	BP clonase	pDONOR221
ZNF295-AS1	NA	pENTR221

Appendix 2: Phenotypic data from Zebrafish screen for 171 clones

Gene Symbol	First conc.	# surviving/ #injected	Second conc.	# surviving/ #injected
ABCG1	10	61/99	50	55/98
ADAMTS1	50	75/100	100	75/100
ADAMTS5	50	87/100	100	84/100
ADARB1	50	62/100	100	79/100
AGPAT3	10	75/100	50	85/100
AIRE	50	81/100	100	87/100
ANKRD20A11P	50	74/100	100	82/100
ANKRD30BP2	10	101/120	50	99/127
APP	10	59/70	50	78/100
ATP5J	10	63/101	50	40/140
ATP5O	10	93/100	50	98/100
B3GALT5	50	92/100	100	99/100
BACE2	50	79/100	100	75/100
BACH1	50	94/100	100	93/100
BAGE	10	39/72	50	79/122
BAGE4	10	104/120	50	100/120
BRWD1	10	29/120	50	35/120
BTG3	10	65/103	50	59/92
C21orf119	50	82/100	100	77/100
C21orf125	10	43/95	50	65/92
C21orf128	50	62/89	100	58/90
C21orf2	50	89/100	100	81/100
C21orf37	10	75/100	50	75/100
C21orf49	10	42/100	50	49/100
C21orf59	10	121/146	50	98/126
C21orf67	50	76/100	100	88/100
C21orf77	10	0/106	50	34/82
C21orf88	50	84/100	100	78/100
C21orf91	10	162/220	50	109/138
C2CD2	10	55/110	50	45/110
CBR1	10	77/100	50	71/100
CBR3	10	51/115	50	52/124
CBS	10	54/117	50	52/106
CCT8	10	60/77	50	83/100
CHAF1B	10	85/100	50	63/100

Appendix 2: Phenotypic data from Zebrafish screen for 171 clones

Gene Symbol	First conc.	# surviving/ #injected	Second conc.	# surviving/ #injected
CHODL	10	56/142	50	63/125
CLDN14	10	2/120	50	0/120
CLDN17	10	93/120	50	68/120
CLDN8	50	92/100	100	66/100
CLIC6	50	87/100	100	64/100
Col18a1	50	92/100	100	97/100
Col6a1	50	99/100	100	87/100
COL6A2	10	69/100	50	72/100
CRYAA	10	28/86	50	13/109
CRYZL1	10	80/100	50	74/100
CSTB	10	71/100	50	71/100
CXADR	10	76/100	50	74/100
CYYR1	50	78/100	100	94/100
DIP2A	10	80/110	50	77/110
DNAJC28	10	77/100	50	85/100
DNMT3L	10	84/100	50	82/100
DONSON	50	92/100	100	84/100
DOPEY2	50	72/100	100	94/100
DSCAM	50	96/100	100	95/100
DSCR10	50	80/100	100	86/100
DSCR3	50	89/100	100	86/100
DSCR4	10	65/95	50	50/83
DSCR8	10	57/135	50	74/150
DSCR9	10	67/130	50	49/113
DYRK1A	50	97/100	100	95/100
ERG	10	22/67	50	7/50
ETS2	10	46/100	50	52/100
EVA1C	10	61/120	50	19/120
FAM207A	10	77/100	50	74/100
FAM3B	10	33/110	50	28/110
FTCD	50	71/100	100	85/100
GABPA	10	0/120	50	75/120
GART	10	12/120	50	37/120
GRIK1	50	56/75	100	53/75
HLCS	10	68/100	50	81/103
HMGN1	10	40/120	50	9/120

Appendix 2: Phenotypic data from Zebrafish screen for 171 clones

Gene Symbol	First conc.	# surviving/ #injected	Second conc.	# surviving/ #injected
HSF2BP	10	97/121	50	84/103
HSPA13	10	89/118	50	84/104
HUNK	50	81/100	100	72/100
IFNAR1	10	68/100	50	65/100
IFNAR2	10	74/110	50	70/110
IFNGR2	10	84/161	50	69/134
IGSF5	50	87/100	100	76/100
IL10RB	10	72/100	50	77/100
ITGB2	10	43/109	50	53/81
ITSN1	50	100/100	100	94/100
JAM2	50	77/100	100	69/100
KCNE1	10	27/50	50	0/50
KCNE2	50	76/100	100	74/100
KCNJ15	10	94/114	50	84/110
KCNJ6	10	83/100	50	79/100
LCA5L	50	95/100	100	92/100
LINC00313 (C21orf84)	10	54/120	50	74/120
LINC00314 (C21orf94)	10	78/103	50	83/110
LINC00478 (C21orf34)	10	76/120	50	71/120
LIPI	50	54/75	100	60/75
LRRC3	50	96/100	100	92/100
LSS	50	78/100	100	79/100
LTN1	50	96/100	100	89/100
MAP3K7CL	10	76/100	50	74/100
MCM3AP 3'	50	72/100	100	88/100
MCM3AP long	50	81/100	100	96/100
MIS18A	10	71/115	50	56/119
MRAP	10	0/120	50	18/102
MRPL39	50	94/100	100	80/100
MRPS6	10	20/73	50	3/103
MX1	50	87/100	100	75/100
MX2	50	88/100	100	88/100
N6AMT1	10	12/120	50	2/120
NCAM2	10	79/100	50	87/100

Appendix 2: Phenotypic data from Zebrafish screen for 171 clones

Gene Symbol	First conc.	# surviving/ #injected	Second conc.	# surviving/ #injected
NDUFV3	10	67/100	50	77/100
NRIP1	50	64/100	100	60/98
OLIG1	10	76/110	50	68/100
OLIG2	50	65/100	100	69/100
PAXBP1	10	21/120	50	24/120
PCBP3	10	78/143	50	71/117
PCP4	10	60/114	50	76/127
PDE9A	10	71/98	50	70/100
PDXK	10	98/125	50	109/137
PFKL	10	79/100	50	69/100
PIGP	10	83/100	50	88/100
PKNOX1	10	71/100	50	69/100
PLAC4	50	90/100	100	93/100
POFUT2	10	144/170	50	163/180
PRDM15	10	41/110	50	70/110
PRMT2	10	81/100	50	84/100
PSMG1	10	54/120	50	22/120
PTTG1IP	10	55/100	50	61/100
PWP2	10	73/111	50	38/80
RBM11	10	57/100	50	48/100
RCAN1	10	71/128	50	18/107
RIPK4	50	90/100	100	86/100
RIPPLY3	10	76/120	50	85/120
RRP1	10	73/114	50	67/96
RSPH1	50	79/100	100	79/100
RUNX1	50	84/100	100	86/100
RWDD2B	10	75/100	50	91/100
S100B	10	71/101	50	93/135
SAMSN1	10	62/100	50	57/100
SCAF4	10	1/120	50	0/120
SETD4	10	0/115	50	11/45
SH3BGR	10	68/120	50	73/120
SIK1	10	17/46	50	70/90
SIM2	50	90/100	100	80/100
SLC19A1	10	91/113	50	67/95
SLC37A1	50	87/100	100	85/100

Appendix 2: Phenotypic data from Zebrafish screen for 171 clones

Gene Symbol	First conc.	# surviving/ #injected	Second conc.	# surviving/ #injected
SLC5A3	10	80/100	50	62/100
SMIM11	10	40/50	50	45/50
SOD1	10	93/100	50	87/100
SPATC1L	10	57/100	50	64/100
SUMO3	10	33/55	50	93/140
SYNJ1-145	50	92/100	100	95/100
SYNJ1-170	50	74/100	100	82/100
TCP10L	10	36/120	50	37/120
TFF1	50	86/99	100	81/98
TFF2	10	75/96	50	103/134
TFF3	10	15/115	50	10/100
TIAM1	50	99/100	100	97/100
TMEM50B	10	50/120	50	40/120
TMPRSS15	10	75/100	50	75/100
TMPRSS2	10	83/120	50	57/120
TMPRSS3	10	68/98	50	65/81
TPTE	10	72/96	50	69/88
TRAPPC10	10	74/85	50	60/72
TRPM2	50	71/100	100	82/100
TTC3	50	87/100	100	78/100
U2AF1	10	57/101	50	145/191
UBASH3A	10	47/80	50	72/124
UBE2G2	10	88/126	50	70/97
USP16	10	51/110	50	0/110
USP25	50	92/100	100	92/100
WDR4	10	99/129	50	97/122
WRB	10	90/120	50	65/120
YBEY	10	62/100	50	80/100
ZNF295	50	90/100	100	84/100
ZNF295-AS1	10	85/100	50	84/100

Appendix 2: Phenotypic data from Zebrafish screen for 171 clones

Gene Symbol	Observed Phenotype
ABCG1	
ADAMTS1	
ADAMTS5	
ADARB1	
AGPAT3	
AIRE	
ANKRD20A11P	
ANKRD30BP2	
APP	
ATP5J	
ATP5O	
B3GALT5	
BACE2	
BACH1	3 cyclopia, 3 craniofacial abnormalities @ 100pg
BAGE	
BAGE4	
BRWD1	
BTG3	2 with no jaw, 2 with small eyes @ 10pg
C21orf119	
C21orf125	
C21orf128	
C21orf2	
C21orf37	
C21orf49	
C21orf59	
C21orf67	
C21orf77	
C21orf88	
C21orf91	
C2CD2	
CBR1	
CBR3	5 with abnormal skulls @ 50pg
CBS	
CCT8	12 with abnormal melanocytes
CHAF1B	

Appendix 2: Phenotypic data from Zebrafish screen for 171 clones

Gene Symbol	Observed Phenotype
CHODL	
CLDN14	
CLDN17	
CLDN8	
CLIC6	11 & 10 Usomites at 50 & 100 pg
Col18a1	
Col6a1	5 with jaw abnormalities @ 100pg
COL6A2	
CRYAA	
CRYZL1	
CSTB	
CXADR	
CYYR1	
DIP2A	
DNAJC28	
DNMT3L	
DONSON	
DOPEY2	
DSCAM	
DSCR10	
DSCR3	
DSCR4	
DSCR8	
DSCR9	
DYRK1A	
ERG	
ETS2	
EVA1C	1 with cyclopia, 2 craniofacial abnormalities
FAM207A	
FAM3B	
FTCD	
GABPA	
GART	6 with small heads and close set eyes
GRIK1	
HLCS	
HMGN1	4 with missing melanocytes @ 50pg

Appendix 2: Phenotypic data from Zebrafish screen for 171 clones

Gene Symbol	Observed Phenotype
HSF2BP	
HSPA13	
HUNK	
IFNAR1	11 Usomites @ 50pg
IFNAR2	
IFNGR2	
IGSF5	
IL10RB	
ITGB2	
ITSN1	
JAM2	11 & 13 with edema @ 50 & 100pg
KCNE1	
KCNE2	
KCNJ15	
KCNJ6	
LCA5L	
LINC00313 (C21orf84)	usomites and cyclopia at 100pg
LINC00314 (C21orf94)	
LINC00478 (C21orf34)	
LIPI	
LRRC3	
LSS	
LTN1	
MAP3K7CL	8 Usomites @ 50pg
MCM3AP 3'	
MCM3AP long	
MIS18A	
MRAP	
MRPL39	
MRPS6	
MX1	
MX2	
N6AMT1	
NCAM2	

Appendix 2: Phenotypic data from Zebrafish screen for 171 clones

Gene Symbol	Observed Phenotype
NDUFV3	
NRIP1	
OLIG1	12 with abnormal fins
OLIG2	
PAXBP1	
PCBP3	10 & 7 Usomites @ 10 & 50pg
PCP4	
PDE9A	
PDXK	
PFKL	
PIGP	
PKNOX1	
PLAC4	
POFUT2	2 with cyclopia @ 50pg
PRDM15	
PRMT2	
PSMG1	
PTTG1IP	
PWP2	
RBM11	
RCAN1	
RIPK4	
RIPPLY3	
RRP1	14 Usomites @ 50pg
RSPH1	
RUNX1	
RWDD2B	15 & 20 with Usomites @ 10 & 50pg
S100B	
SAMSN1	3&4 craniofacial abnormalities @ 10 & 50pg
SCAF4	
SETD4	
SH3BGR	
SIK1	
SIM2	
SLC19A1	
SLC37A1	

Appendix 2: Phenotypic data from Zebrafish screen for 171 clones

Gene Symbol	Observed Phenotype
SLC5A3	
SMIM11	
SOD1	30 with Usomites @ 50pg
SPATC1L	7 with reduced pigment in eye
SUMO3	
SYNJ1-145	
SYNJ1-170	
TCP10L	
TFF1	
TFF2	
TFF3	
TIAM1	
TMEM50B	
TMPRSS15	7 with cyclopia @ 50pg
TMPRSS2	
TMPRSS3	
TPTE	
TRAPPC10	
TRPM2	
TTC3	
U2AF1	
UBASH3A	
UBE2G2	
USP16	
USP25	
WDR4	
WRB	
YBEY	15 Usomites @ 50pg
ZNF295	
ZNF295-AS1	

References

1. Esquirol E (1838) Mental Maladies: a Treatise on Insanity. Hunt EK, translator. Philadelphia: Lea and Blanchard.
2. Megarbane A, Ravel A, Mircher C, Sturtz F, Grattau Y, et al. (2009) The 50th anniversary of the discovery of trisomy 21: the past, present, and future of research and treatment of Down syndrome. Genet Med 11: 611-616.
3. Roubertoux PL, Kerdelhue B (2006) Trisomy 21: from chromosomes to mental retardation. Behav Genet 36: 346-354.
4. Down J (1866) Observations on an ethnic classification of idiots. London Hospital Clinical Report 3: 259-262.
5. Epstein CJ, Korenberg JR, Anneren G, Antonarakis SE, Ayme S, et al. (1991) Protocols to establish genotype-phenotype correlations in Down syndrome. Am J Hum Genet 49: 207-235.
6. Antonarakis SE, Epstein CJ (2006) The challenge of Down syndrome. Trends Mol Med 12: 473-479.
7. Antonarakis SE, Lyle R, Dermitzakis ET, Reymond A, Deutsch S (2004) Chromosome 21 and down syndrome: from genomics to pathophysiology. Nat Rev Genet 5: 725-738.
8. Allen G (1974) Aetiology of Down's syndrome inferred by Waardenburg in 1932. Nature 250: 436-437.
9. Davenport CB (1932) Mendelism in Man. Proc 6th Intern Cong Genetics 1: 135-140.

10. Hattori M, Fujiyama A, Taylor TD, Watanabe H, Yada T, et al. (2000) The DNA sequence of human chromosome 21. Nature 405: 311-319.

11. Gardiner K (2003) Predicting pathway perturbations in Down syndrome. J Neural Transm Suppl: 21-37.

12. Sturgeon X, Gardiner KJ (2011) Transcript catalogs of human chromosome 21 and orthologous chimpanzee and mouse regions. Mamm Genome 22: 261-271.

13. Patterson D (2007) Genetic mechanisms involved in the phenotype of Down syndrome. Ment Retard Dev Disabil Res Rev 13: 199-206.

14. Rahmani Z, Blouin JL, Creau-Goldberg N, Watkins PC, Mattei JF, et al. (1989) Critical role of the D21S55 region on chromosome 21 in the pathogenesis of Down syndrome. Proc Natl Acad Sci U S A 86: 5958-5962.

15. Sinet PM, Theophile D, Rahmani Z, Chettouh Z, Blouin JL, et al. (1994) Mapping of the Down syndrome phenotype on chromosome 21 at the molecular level. Biomed Pharmacother 48: 247-252.

16. Korenberg JR, Chen XN, Schipper R, Sun Z, Gonsky R, et al. (1994) Down syndrome phenotypes: the consequences of chromosomal imbalance. Proc Natl Acad Sci U S A 91: 4997-5001.

17. Korbel JO, Tirosh-Wagner T, Urban AE, Chen XN, Kasowski M, et al. (2009) The genetic architecture of Down syndrome phenotypes revealed by high-resolution analysis of human segmental trisomies. Proc Natl Acad Sci U S A 106: 12031-12036.

18. Lyle R, Bena F, Gagos S, Gehrig C, Lopez G, et al. (2009) Genotype-phenotype correlations in Down syndrome identified by array CGH in 30 cases of partial trisomy and partial monosomy chromosome 21. Eur J Hum Genet 17: 454-466.

19. Mural RJ, Adams MD, Myers EW, Smith HO, Miklos GL, et al. (2002) A comparison of whole-genome shotgun-derived mouse chromosome 16 and the human genome. Science 296: 1661-1671.

20. Pletcher MT, Wiltshire T, Cabin DE, Villanueva M, Reeves RH (2001) Use of comparative physical and sequence mapping to annotate mouse chromosome 16 and human chromosome 21. Genomics 74: 45-54.

21. Reeves RH, Garner CC (2007) A year of unprecedented progress in Down syndrome basic research. Ment Retard Dev Disabil Res Rev 13: 215-220.

22. Wiltshire T, Pletcher M, Cole SE, Villanueva M, Birren B, et al. (1999) Perfect conserved linkage across the entire mouse chromosome 10 region homologous to human chromosome 21. Genome Res 9: 1214-1222.

23. Dierssen M, Fillat C, Crnic L, Arbones M, Florez J, et al. (2001) Murine models for Down syndrome. Physiol Behav 73: 859-871.

24. Salehi A, Faizi M, Belichenko PV, Mobley WC (2007) Using mouse models to explore genotype-phenotype relationship in Down syndrome. Ment Retard Dev Disabil Res Rev 13: 207-214.

25. Reeves RH, Irving NG, Moran TH, Wohn A, Kitt C, et al. (1995) A mouse model for Down syndrome exhibits learning and behaviour deficits. Nat Genet 11: 177-184.

26. Starbuck J, Dutka T, Ratliff T, Reeves RH, Richtsmeier JT (In press) Overlapping Trisomies for Human Chromosome 21 Orthologs Produce Similar Effects on

Skull and Brain Morphology of Dp(16)1Yey and Ts65Dn Mice. Am J Med Genet Part A.

27. Roper RJ, Reeves RH (2006) Understanding the basis for Down syndrome phenotypes. PLoS Genet 2: e50.

28. Richtsmeier JT, Baxter LL, Reeves RH (2000) Parallels of craniofacial maldevelopment in Down syndrome and Ts65Dn mice. Dev Dyn 217: 137-145.

29. Olson LE, Roper RJ, Baxter LL, Carlson EJ, Epstein CJ, et al. (2004) Down syndrome mouse models Ts65Dn, Ts1Cje, and Ms1Cje/Ts65Dn exhibit variable severity of cerebellar phenotypes. Dev Dyn 230: 581-589.

30. Gardiner K, Herault Y, Lott IT, Antonarakis SE, Reeves RH, et al. (2010) Down syndrome: from understanding the neurobiology to therapy. J Neurosci 30: 14943-14945.

31. Garcia MD, Udan RS, Hadjantonakis AK, Dickinson ME (2011) Live imaging of mouse embryos. Cold Spring Harb Protoc 2011: pdb top104.

32. Garcia MD, Udan RS, Hadjantonakis AK, Dickinson ME (2011) Time-lapse imaging of postimplantation mouse embryos. Cold Spring Harb Protoc 2011: pdb prot5595.

33. Schilling TF, Webb J (2007) Considering the zebrafish in a comparative context. J Exp Zool B Mol Dev Evol 308: 515-522.

34. Rinkwitz S, Mourrain P, Becker TS (2011) Zebrafish: an integrative system for neurogenomics and neurosciences. Prog Neurobiol 93: 231-243.

35. Villefranc JA, Amigo J, Lawson ND (2007) Gateway compatible vectors for analysis of gene function in the zebrafish. Dev Dyn 236: 3077-3087.

36. Yelick PC, Schilling TF (2002) Molecular dissection of craniofacial development using zebrafish. Crit Rev Oral Biol Med 13: 308-322.

37. Jin SW, Herzog W, Santoro MM, Mitchell TS, Frantsve J, et al. (2007) A transgene-assisted genetic screen identifies essential regulators of vascular development in vertebrate embryos. Dev Biol 307: 29-42.

38. Scott EK, Baier H (2009) The cellular architecture of the larval zebrafish tectum, as revealed by gal4 enhancer trap lines. Front Neural Circuits 3: 13.

39. Katzen F (2007) Gateway((R)) recombinational cloning: a biological operating system. Expert Opin Drug Discov 2: 571-589.

40. (2002) The NCBI handbook [Internet]. Bethesda (MD) National Library of Medicine (US), National Center for Biotechnology Information.

41. Dutta S, Nandagopal K, Gangopadhyay PK, Mukhopadhyay K (2005) Molecular aspects of Down syndrome. Indian Pediatr 42: 339-344.

42. Westerfield M (2000) The Zebrafish Book: a guide for the laboratory use of zebrafish (*Danio rerio*). Eugene, OR: University of Oregon Press.

43. Powell GT, Wright GJ (2011) Jamb and jamc are essential for vertebrate myocyte fusion. PLoS Biol 9: e1001216.

44. Reymond A, Marigo V, Yaylaoglu MB, Leoni A, Ucla C, et al. (2002) Human chromosome 21 gene expression atlas in the mouse. Nature 420: 582-586.

45. Armit C, Venkataraman S, Richardson L, Stevenson P, Moss J, et al. (2012) eMouseAtlas, EMAGE, and the spatial dimension of the transcriptome. Mamm Genome 23: 514-524.

46. Cunningham SA, Arrate MP, Rodriguez JM, Bjercke RJ, Vanderslice P, et al. (2000) A novel protein with homology to the junctional adhesion molecule. Characterization of leukocyte interactions. J Biol Chem 275: 34750-34756.

47. Gitton Y, Dahmane N, Baik S, Ruiz i Altaba A, Neidhardt L, et al. (2002) A gene expression map of human chromosome 21 orthologues in the mouse. Nature 420: 586-590.

48. Kahlem P, Sultan M, Herwig R, Steinfath M, Balzereit D, et al. (2004) Transcript level alterations reflect gene dosage effects across multiple tissues in a mouse model of down syndrome. Genome Res 14: 1258-1267.

49. Hu YH, Warnatz HJ, Vanhecke D, Wagner F, Fiebitz A, et al. (2006) Cell array-based intracellular localization screening reveals novel functional features of human chromosome 21 proteins. BMC Genomics 7: 155.

50. Joshi P, Greco TM, Guise AJ, Luo Y, Yu F, et al. (2013) The functional interactome landscape of the human histone deacetylase family. Mol Syst Biol 9: 672.

51. Miura T, Nishinaka T, Terada T (2008) Different functions between human monomeric carbonyl reductase 3 and carbonyl reductase 1. Mol Cell Biochem 315: 113-121.

52. Ludwig RJ, Hardt K, Hatting M, Bistrian R, Diehl S, et al. (2009) Junctional adhesion molecule (JAM)-B supports lymphocyte rolling and adhesion through interaction with alpha4beta1 integrin. Immunology 128: 196-205.

53. Stelzl U, Worm U, Lalowski M, Haenig C, Brembeck FH, et al. (2005) A human protein-protein interaction network: a resource for annotating the proteome. Cell 122: 957-968.

54. Varjosalo M, Keskitalo S, Van Drogen A, Nurkkala H, Vichalkovski A, et al. (2013) The protein interaction landscape of the human CMGC kinase group. Cell Rep 3: 1306-1320.

55. Wang J, Yuan Y, Zhou Y, Guo L, Zhang L, et al. (2008) Protein interaction data set highlighted with human Ras-MAPK/PI3K signaling pathways. J Proteome Res 7: 3879-3889.

56. Savino TM, Bastos R, Jansen E, Hernandez-Verdun D (1999) The nucleolar antigen Nop52, the human homologue of the yeast ribosomal RNA processing RRP1, is recruited at late stages of nucleologenesis. J Cell Sci 112 (Pt 12): 1889-1900.

57. Gardiner K, Davisson MT, Crnic LS (2004) Building protein interaction maps for Down's syndrome. Brief Funct Genomic Proteomic 3: 142-156.

58. Du J, Takeuchi H, Leonhard-Melief C, Shroyer KR, Dlugosz M, et al. (2010) O-fucosylation of thrombospondin type 1 repeats restricts epithelial to mesenchymal transition (EMT) and maintains epiblast pluripotency during mouse gastrulation. Dev Biol 346: 25-38.

59. Peled-Kamar M, Lotem J, Wirguin I, Weiner L, Hermalin A, et al. (1997) Oxidative stress mediates impairment of muscle function in transgenic mice with elevated level of wild-type Cu/Zn superoxide dismutase. Proc Natl Acad Sci U S A 94: 3883-3887.

60. Avraham KB, Schickler M, Sapoznikov D, Yarom R, Groner Y (1988) Down's syndrome: abnormal neuromuscular junction in tongue of transgenic mice with elevated levels of human Cu/Zn-superoxide dismutase. Cell 54: 823-829.

61. Avraham KB, Sugarman H, Rotshenker S, Groner Y (1991) Down's syndrome: morphological remodelling and increased complexity in the neuromuscular junction of transgenic CuZn-superoxide dismutase mice. J Neurocytol 20: 208-215.

62. Atkin JD, Scott RL, West JM, Lopes E, Quah AK, et al. (2005) Properties of slow- and fast-twitch muscle fibres in a mouse model of amyotrophic lateral sclerosis. Neuromuscul Disord 15: 377-388.

63. Garrett AM, Tadenev AL, Burgess RW (2012) DSCAMs: restoring balance to developmental forces. Front Mol Neurosci 5: 86.

64. Grossman TR, Gamliel A, Wessells RJ, Taghli-Lamallem O, Jepsen K, et al. (2011) Over-expression of DSCAM and COL6A2 cooperatively generates congenital heart defects. PLoS Genet 7: e1002344.

65. Dierssen M, de Lagran MM (2006) DYRK1A (dual-specificity tyrosine-phosphorylated and -regulated kinase 1A): a gene with dosage effect during development and neurogenesis. ScientificWorldJournal 6: 1911-1922.

66. Dierssen M, Herault Y, Estivill X (2009) Aneuploidy: from a physiological mechanism of variance to Down syndrome. Physiol Rev 89: 887-920.

67. De la Torre R, De Sola S, Pons M, Duchon A, de Lagran MM, et al. (2014) Epigallocatechin-3-gallate, a DYRK1A inhibitor, rescues cognitive deficits in Down syndrome mouse models and in humans. Mol Nutr Food Res 58: 278-288.

68. Golzio C, Willer J, Talkowski ME, Oh EC, Taniguchi Y, et al. (2012) KCTD13 is a major driver of mirrored neuroanatomical phenotypes of the 16p11.2 copy number variant. Nature 485: 363-367.

69. Takeda H, Matsuzaki T, Oki T, Miyagawa T, Amanuma H (1994) A novel POU domain gene, zebrafish pou2: expression and roles of two alternatively spliced twin products in early development. Genes Dev 8: 45-59.

70. Currier DG, Polk RC, Reeves RH (2012) A Sonic hedgehog (Shh) response deficit in trisomic cells may be a common denominator for multiple features of Down syndrome. Prog Brain Res 197: 223-236.

71. Bryson-Richardson RJ, Currie PD (2008) The genetics of vertebrate myogenesis. Nat Rev Genet 9: 632-646.

72. Wolff C, Roy S, Ingham PW (2003) Multiple muscle cell identities induced by distinct levels and timing of hedgehog activity in the zebrafish embryo. Curr Biol 13: 1169-1181.

73. Stickney HL, Barresi MJ, Devoto SH (2000) Somite development in zebrafish. Dev Dyn 219: 287-303.

74. van Eeden FJ, Granato M, Schach U, Brand M, Furutani-Seiki M, et al. (1996) Mutations affecting somite formation and patterning in the zebrafish, Danio rerio. Development 123: 153-164.

75. Nasevicius A, Ekker SC (2000) Effective targeted gene 'knockdown' in zebrafish. Nat Genet 26: 216-220.

76. Roper RJ, Baxter LL, Saran NG, Klinedinst DK, Beachy PA, et al. (2006) Defective cerebellar response to mitogenic Hedgehog signaling in Down [corrected] syndrome mice. Proc Natl Acad Sci U S A 103: 1452-1456.

77. Roper RJ, VanHorn JF, Cain CC, Reeves RH (2009) A neural crest deficit in Down syndrome mice is associated with deficient mitotic response to Sonic hedgehog. Mech Dev 126: 212-219.

78. Aanstad P, Santos N, Corbit KC, Scherz PJ, Trinh le A, et al. (2009) The extracellular domain of Smoothened regulates ciliary localization and is required for high-level Hh signaling. Curr Biol 19: 1034-1039.

79. Jenkins D (2009) Hedgehog signalling: emerging evidence for non-canonical pathways. Cell Signal 21: 1023-1034.

80. Vaillant C, Monard D (2009) SHH pathway and cerebellar development. Cerebellum 8: 291-301.

81. Bijlsma MF, Damhofer H, Roelink H (2012) Hedgehog-stimulated chemotaxis is mediated by smoothened located outside the primary cilium. Sci Signal 5: ra60.

82. Trazzi S, Mitrugno VM, Valli E, Fuchs C, Rizzi S, et al. (2011) APP-dependent up-regulation of Ptch1 underlies proliferation impairment of neural precursors in Down syndrome. Hum Mol Genet 20: 1560-1573.

83. Maroto M, Bone RA, Dale JK (2012) Somitogenesis. Development 139: 2453-2456.

84. Kimmel CB, Ballard WW, Kimmel SR, Ullmann B, Schilling TF (1995) Stages of embryonic development of the zebrafish. Dev Dyn 203: 253-310.

85. Marcelle C, Ahlgren S, Bronner-Fraser M (1999) In vivo regulation of somite differentiation and proliferation by Sonic Hedgehog. Dev Biol 214: 277-287.

86. Svetic V, Hollway GE, Elworthy S, Chipperfield TR, Davison C, et al. (2007) Sdf1a patterns zebrafish melanophores and links the somite and melanophore pattern defects in choker mutants. Development 134: 1011-1022.

CURRICULUM VITAE

SARAH MCGUIRE EDIE

3610 Malden Ave, Baltimore, MD 21211

C: 719-331-0560 sedie@jhmi.edu

Born May 20, 1982 in Newburyport, MA

EDUCATION

B.A. 2005	Biological Sciences Wellesley College, Wellesley MA
PhD 2014	Pre-doctoral Training Program in Human Genetics Johns Hopkins University, School of Medicine, Baltimore, MD Laboratory of Roger H. Reeves, Ph.D. Thesis title: "Effects of Hsa21 gene expression on early vertebrate development." Seminar presented January 31, 2014

RESEARCH EXPERIENCE

June 2008-present	Graduate Student, Johns Hopkins University

Used zebrafish as a model system for over expressing genes from human chromosome 21 to understand the basis of Down Syndrome phenotypes.

June 2005-August 2007 Senior Lab Technician, Johns Hopkins University

Studied a rare genetic disease, Albright Hereditary Osteodystrophy, using human populations to understand the effects of epigenetic imprinting on phenotype presentation and a mouse model to examine the subcutaneous ossification phenotype.

June 2004-August 2004 Summer Internship, Wellesley College

Used Mass Spec to analyze the calmodulin protein in Arabidopsis thaliana.

TEACHING EXPERIENCE

Nov. 2011-Dec. 2011 Teaching Assistant for graduate school course:

Fundamentals of Human Genetics (85 students).

Wrote and graded problem set and exam questions.

January 2010-June 2010 Teaching Assistant for graduate school course:

Advanced Topics in Human Genetics (16 students).

Lead weekly discussion groups, wrote and graded exam.

PUBLICATIONS

Edie S, Zaghloul N, Klinedinst D, Lebron J, Katsanis N, Reeves RH.

Effects of over expression of Hsa21 genes on early development. (In preparation)

DL Huso, S Edie, MA Levine, W Schwindinger, Y Wang, H Jüppner, EL Germain-Lee. Heterotopic ossifications in a mouse model of Albright hereditary osteodystrophy.

PloS One 2011 ;6(6):e21755.

AZ Moore, ML Biggs, A Matteini, A O'Connor, S McGuire, BA Beamer, MD Fallin, LP Fried, J Walston, A Chakravarti, DE Arking. Polymorphisms in the mitochondrial DNA control region and frailty in older adults.

PLoS One 2010 Jun 10;5(6):e11069

DN Long, S McGuire, MA Levine, LS Weinstein, EL Germain-Lee. Body mass index differences in pseudohypoparathyroidism type 1a versus pseudopseudohypoparathyroidism may implicate paternal imprinting of Galpha(s) in the development of human obesity.

J Clin Endocrinol Metab. 2007 Mar;92(3):1073-9.

PRESENTATIONS

Pair wise combinatorial injections of Hsa21 genes show a synthetic dosage effect on Shh-related phenotypes in zebrafish

Edie S, Zaghloul N, Klinedinst D, Lebron J, Katsanis N, Reeves RH.

POSTER presented at the Workshop on Cognition in Down Syndrome, April 14, 2013

Dosage effects of 169 Chr21 genes on early development events in Zebrafish

S Edie, N Zaghloul, D Klinedinst, J Lebron, N Katsanis, R Reeves.

PLATFORM talk, presented at the 62nd Annual Meeting of The American Society of Human Genetics, November 9, 2012

Mitochondrial D-loop genetic variation is associated with frailty in Caucasians from the Cardiovascular Health Study (CHS). S McGuire, M.L. Biggs, A.L. Rea, A. O'Connor, B. Beamer, M.D. Fallin, A. Chakravarti, L.P. Fried, J. Walston, D.E. Arking.

POSTER presented at the 58th Annual Meeting of The American Society of Human Genetics, November 11, 2008.

Heterotopic Subcutaneous Ossifications in a Mouse Model of Albright Hereditary Osteodystrophy. DL Huso, S McGuire and EL Germain-Lee.

POSTER presented at the Endocrine Society's 89th annual meeting, June 5, 2007.

AWARDS

Graduate Student Association of Johns Hopkins University Travel Award 2012